Recursive algorithms for estimating the parameters in a one dimensional heat diffusion system: analysis

Bharath Bhikkaji*, Kaushik Mahata* and Torsten Söderström*

Abstract

In [5], we have proposed two recursive algorithms in the frequency domain to estimate the parameters of a one dimensional heat diffusion system. There in, we have discussed in detail the construction and the implementation of the algorithms. Further in [5], we observed the convergence of the proposed algorithms using certain numerical examples. In this paper, we analyse the convergence of these algorithms from a theoretical perspective.

Keywords: Circular convolution, convergence analysis, convolution, frequency domain, heat diffusion, infinite dimensional system, recursive algorithms.

*Division of Systems and Control, Department of Information Technology, Uppsala University, P O Box 337, SE 75105, Uppsala, Sweden, email bb@it.uu.se, km@it.uu.se, ts@it.uu.se

1 Introduction

In the recent past, we have considered the problem of estimating the parameters involved in a one dimensional heat diffusion system, see [5], [6], [7], [8], [11] and [14]. Heat diffusion systems, in general, are modeled by partial differential equations (PDEs) involving certain parameters. To get a complete description of a given heat diffusion system, one has to either know or determine the parameters involved in the corresponding PDE model. In [11] and [14] we have estimated the parameters of a one dimensional heat diffusion system using the standard output error method, see [16], which is a batch estimation technique. In [7], under certain conditions, we have provided a proof for the convergence of the parameter estimates obtained in [11] and [14], to their respective true parameter values. Recursive estimation of the parameters of a one dimensional heat diffusion system was considered in [5] and [8]. In [8] the recursive estimation was performed using the standard recursive prediction error method (RPEM), see [16]. In [5] we have proposed two new recursive algorithms, which are defined in the frequency domain, to estimate the parameters. In [5] the convergence of the parameters estimates generated by the proposed recursive algorithms were observed by considering a numerical example. Here we analyse their convergence from a theoretical perspective.

2 Problem description

As in [5], [14] and [15], we consider a one dimensional heat diffusion across a homogeneous wall of length d units. Let $T(x,t)$ denote the temperature profile across the wall with abscissa x, at time t, $T_e(t)$ denote the exterior temperature, $T_i(t) \triangleq T(0,t)$ denote the interior temperature, and $q_i(t)$ denote the heat supplied form the interior. The dynamics of $T(x,t)$ is governed by the PDE

$$\frac{\partial T(x,t)}{\partial t} = \alpha_0 \frac{\partial^2 T(x,t)}{\partial x^2}, \quad 0 < x < d \tag{1}$$

with boundary constraints

$$q_i(t) = -\kappa_0 \frac{\partial T(x,t)}{\partial x} \Big|_{x=0}, \tag{2}$$

$$T_e(t) = T(d,t), \tag{3}$$

and initial condition

$$T(x,0) = 0, \quad 0 \le x \le d, \tag{4}$$

where α_0 and κ_0, the diffusion coefficient and the thermal conductivity respectively, are the unknown parameters which characterise the wall. Since the chosen wall is homogeneous, the parameters α_0 and κ_0 are constants. Further, by nature, all materials have strictly positive diffusion coefficients and thermal conductivities.

The estimation problem considered here is the following:

Given: At any instant $t = Nh$, the sampled data
$Y^N = \left\{q_i^H(kh), T_i^H(kh), T_e^H(kh)\right\}_{k=0}^{N-1}$, for a known sampling interval h.

Estimate: The parameters α_0 and κ_0 recursively in time.

Here, the signals $q_i^H(t), T_i^H(t)$ and $T_e^H(t)$ denote the outputs of an anti-aliasing filter (AA filter, from now on) $H(\mathrm{i}\Omega)$ corresponding to the inputs $q_i(t), T_i(t)$ and $T_e(t)$, respectively. Since the signals are sampled at an interval h, it is a standard practice to assume that $q_i(t), T_i(t)$ and $T_e(t)$ are filtered using a band limited[1] AA filter with a cutoff $\Omega_c < \frac{\pi}{h}$ rads/sec before sampling, see [2] and [4]. Pre-filtering $q_i(t), T_i(t)$ and $T_e(t)$ using $H(\mathrm{i}\Omega)$, and sampling the corresponding filter outputs avoids aliasing in the sampled data $\{q_i^H(kh), T_i^H(kh), T_e^H(kh)\}_{k=0}^{N-1}$. Details on the pre-filtering and its effect on the chosen estimation problem are discussed in the next section.

3 Perceived dynamics

In this section, we present a characterization of the system dynamics as seen from the given data $\{q_i^H(kh), T_i^H(kh), T_e^H(kh)\}_{k=0}^{\infty}$.

In [14] and [15], we have shown that the given diffusion system, (1)-(4), can be interpreted as an LTI system with inputs

$$u(t) \triangleq [q_i(t)\ , T_e(t)]^\top, \tag{5}$$

and the output

$$\begin{aligned} y(t) &\triangleq T(0,t) \\ &= T_i(t). \end{aligned} \tag{6}$$

In particular, in [14] and [15] it has been shown that (1)-(4) can be re-written in the Laplace domain as

$$Y(s) = G(s, \theta_0)U(s), \tag{7}$$

[1] A band limited signal is a signal whose frequency response is zero beyond a certain frequency known as the cutoff frequency.

where $Y(s)$ and $U(s)$ are the Laplace transforms of the output $y(t)$ and the input $u(t)$ respectively, and the transfer-function $G(s,\theta_0)$ is given by

$$
\begin{aligned}
G(s,\theta_0) &= \left[\frac{\tanh(d\sqrt{\frac{s}{\alpha_0}})}{\kappa_0\sqrt{\frac{s}{\alpha_0}}}\,,\,\frac{1}{\cosh(d\sqrt{\frac{s}{\alpha_0}})}\right] \\
&\triangleq [G_1(s,\theta_0), G_2(s,\theta_0)] \qquad (8)
\end{aligned}
$$

with

$$\theta_0 = (\alpha_0, \kappa_0). \qquad (9)$$

Note that both $G_1(s,\theta_0)$ and $G_2(s,\theta_0)$ have the same set of poles, see [14] and [15],

$$p_n = -\frac{\pi^2}{d^2}(n-\frac{1}{2})^2\alpha_0, \quad n = 1,2,3,\ldots \qquad (10)$$

which are strictly negative. And only $G_1(s,\theta_0)$ has zeros, namely at

$$z_n = -\frac{\pi^2}{d^2}n^2\alpha_0 \quad n = 1,2,3,\ldots. \qquad (11)$$

Since the poles are strictly negative the chosen diffusion system is *bounded input bounded output* (BIBO) stable.

As mentioned earlier, the system input $u(t)$, (5), and the system output $y(t)$, (6), are first filtered using an anti-aliasing filter (AA filter), $H(\mathrm{i}\Omega)$, and the corresponding filter outputs $u_H(t)$ and $y_H(t)$ are then sampled to obtain the given data

$$
\begin{aligned}
u_d(k) &\triangleq u_H(kh) \\
&= \left[q_i^H(kh), T_e^H(kh)\right]^\top, \quad k = 0,1,2,\ldots, \qquad (12)
\end{aligned}
$$

and

$$
\begin{aligned}
y_d(k) &\triangleq y_H(kh) \\
&= T_i^H(kh), \quad k = 0,1,2,\ldots, \qquad (13)
\end{aligned}
$$

respectively, see Figure 1. Here, one must take note of the fact that AA filters are also BIBO stable systems. Since the Fourier transforms of the filtered signals $u_H(t)$ and $y_H(t)$ are

$$U_H(\mathrm{i}\Omega) = U(\mathrm{i}\Omega)H(\mathrm{i}\Omega) \qquad (14)$$

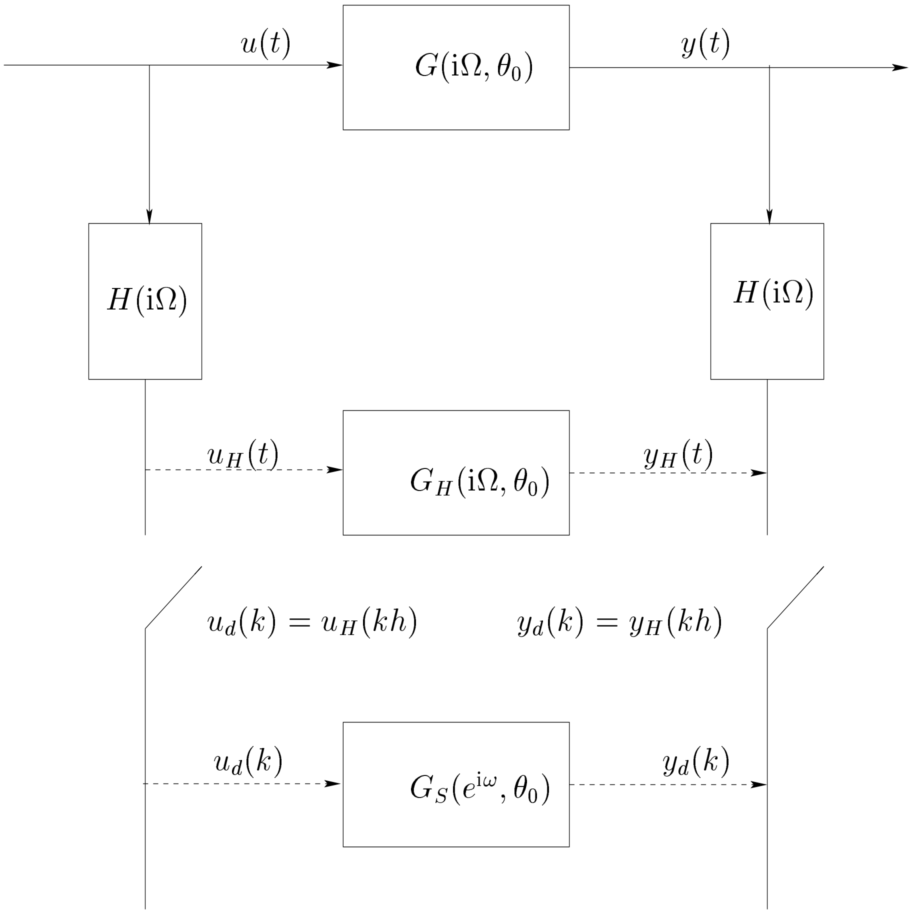

Figure 1: Schematic diagram of pre-filtering and sampling of the input $u(t)$ and output $y(t)$.

and

$$Y_H(\mathrm{i}\Omega) \;=\; Y(\mathrm{i}\Omega)H(\mathrm{i}\Omega) \tag{15}$$

respectively, the frequency response function (FRF), $G_H(\mathrm{i}\Omega, \theta_0)$, of the filtered signals, defined by

$$Y_H(\mathrm{i}\Omega) \;\triangleq\; G_H(\mathrm{i}\Omega, \theta_0)U_H(\mathrm{i}\Omega), \tag{16}$$

is

$$G_H(\mathrm{i}\Omega, \theta_0) \;=\; G(\mathrm{i}\Omega, \theta_0), \quad \mid \Omega \mid < \Omega_c. \tag{17}$$

and not defined for $\mid \Omega \mid \geq \Omega_c$. See (a) and (b) in Figures 2, 3 and 4 for an illustration.

So far, we have only determined the FRF, $G_H(i\Omega,\theta_0)$, corresponding to filtered signals $u_H(t)$ and $y_H(t)$. We now determine the FRF characterised the sampled signals $\{u_d(k)\}_{k=0}^{\infty}$ and $\{y_d(k)\}_{k=0}^{\infty}$. Let $U_S(e^{\mathrm{i}\omega})$ and $Y_S(e^{\mathrm{i}\omega})$ denote the Discrete Fourier transforms (DFT) of the signals $\{u_d(k)\}_{k=0}^{\infty}$ and $\{y_d(k)\}_{k=0}^{\infty}$, respectively. From the standard Shannon sampling theorem, see [2], [9] or [13], we know that

$$hU_S(e^{\mathrm{i}\omega}) = U_H\left(\mathrm{i}\frac{\omega}{h}\right) + \sum_{k=-\infty,\, k\neq 0}^{\infty} U_H\left(\mathrm{i}\,\frac{\omega-2\pi k}{h}\right) \tag{18}$$

and

$$hY_S(e^{\mathrm{i}\omega}) = Y_H\left(\mathrm{i}\frac{\omega}{h}\right) + \sum_{k=-\infty,\, k\neq 0}^{\infty} Y_H\left(\mathrm{i}\,\frac{\omega-2\pi k}{h}\right). \tag{19}$$

Here, in (18) and (19), we have denoted the frequency variable by ω, which is expressed in rads, in order to distinguish it from its continuous time counterpart Ω, which is expressed in rads/sec.

Consider the DFT $U_S(e^{\mathrm{i}\omega})$. Since $U_S(e^{\mathrm{i}\omega})$ is periodic with period 2π, it is enough if one knows, or determines, $U_S(e^{\mathrm{i}\omega})$ in the interval $[-\pi,\pi]$. As $U_H\left(\mathrm{i}\frac{\omega}{h}\right)$ is zero beyond $\mid \frac{\omega}{h} \mid\geq \Omega_c$, where $\Omega_c < \frac{\pi}{h}$, from (18) we have

$$U_S(e^{\mathrm{i}\omega}) = \begin{cases} \frac{1}{h}U_H\left(\mathrm{i}\frac{\omega}{h}\right) & \mid\omega\mid <\ \Omega_c h \\ 0 & \Omega_c h\ <\mid\ \omega\mid <\ \pi, \end{cases} \tag{20}$$

in the interval $[-\pi,\pi]$. See (c) in Figure 2 for an illustration. Similarly, it can be inferred that $Y_S(e^{\mathrm{i}\omega})$ is

$$Y_S(e^{\mathrm{i}\omega}) = \begin{cases} \frac{1}{h}Y_H\left(\mathrm{i}\frac{\omega}{h}\right) & \mid\omega\mid <\ \Omega_c h \\ 0 & \Omega_c h\ <\mid\ \omega\mid <\ \pi. \end{cases} \tag{21}$$

in the interval $[-\pi,\pi]$. See (c) in Figure 3 for an illustration. Therefore the FRF, $G_S(e^{\mathrm{i}\omega},\theta_0)$, corresponding to the sampled signals $\{u_d(k)\}_{k=0}^{\infty}$ and $\{y_d(k)\}_{k=0}^{\infty}$, which is defined by

$$Y_S(e^{\mathrm{i}\omega}) \ \triangleq\ G_S(e^{\mathrm{i}\omega},\theta_0)U_S(e^{\mathrm{i}\omega}), \tag{22}$$

is periodic with period 2π, and equal to

$$G_S(e^{\mathrm{i}\omega},\theta_0) = \ G_H\left(\mathrm{i}\tfrac{\omega}{h},\theta_0\right) \qquad \mid\omega\mid <\ \Omega_c h \tag{23}$$

and not defined for $\Omega_c h\ <\mid\ \omega\mid <\ \pi$. See (c) in Figure 4 for an illustration.

auto-regressive moving average (ARMA) p

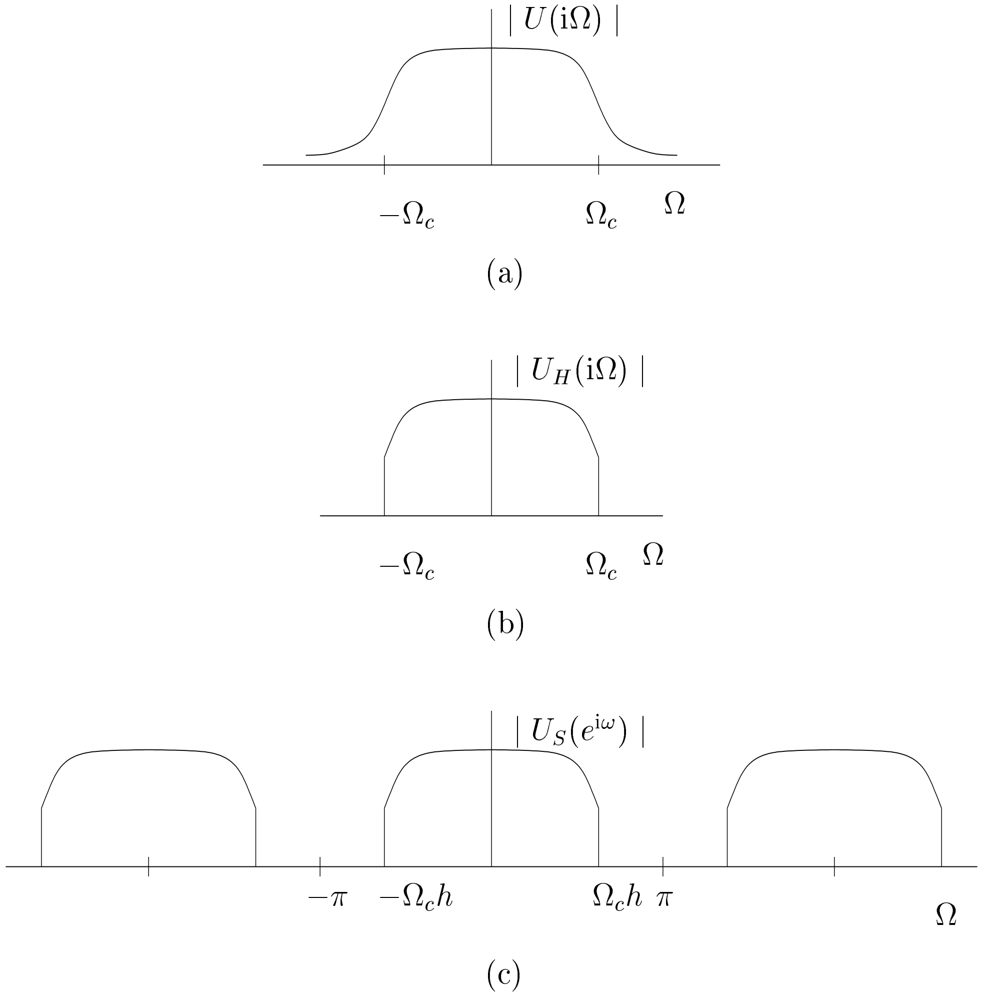

Figure 2: Schematic pictures of the Fourier transforms of (a) $u(t)$, the system input, (b) $u_H(t)$, system input pre-filtered with $H(\mathrm{i}\Omega)$ and (c) $u_d(k)$, the pre-filtered and sampled input.

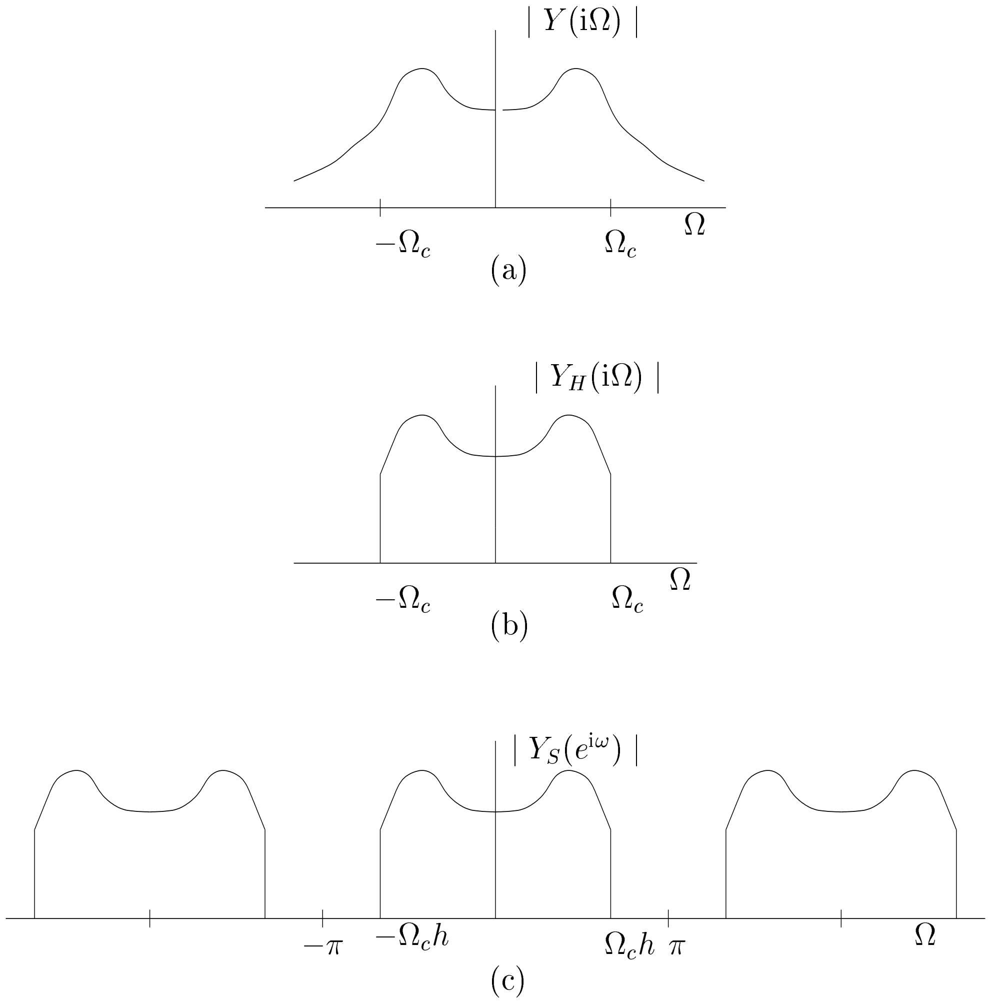

Figure 3: Schematic pictures of the Fourier transforms of (a) $y(t)$, the system output, (b) $y_H(t)$, system output pre-filtered with $H(\mathrm{i}\Omega)$ and (c) $y_d(k)$, the pre-filtered and sampled output.

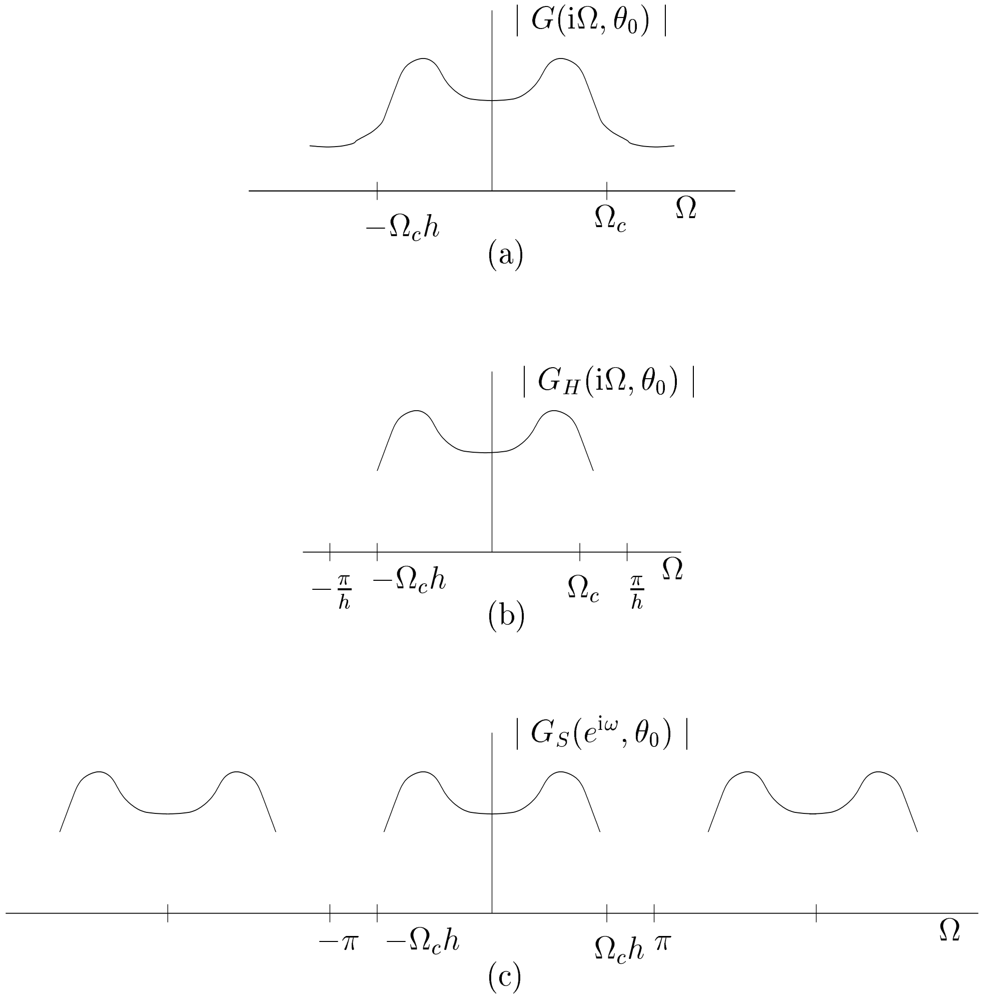

Figure 4: Schematic pictures of (a) the system frequency response function (FRF) $G(\mathrm{i}\Omega, \theta_0)$, (b) The FRF of the filtered data $G_H(\mathrm{i}\Omega.\theta_0)$ and (c) The FRF of the sampled data $G_S(\mathrm{i}\Omega, \theta_0))$.

4 Recursive algorithms in the frequency domain

In this section, we give a brief description of the Frequency domain recursive algorithm (FD-R) and the Windowed frequency domain recursive algorithm (WFD-R), which were proposed in [5] to estimate the parameters α_0 and κ_0 recursively in time.

4.1 Frequency Domain Recursive Algorithm (FD-R)

Consider the following windowed data $\{y_d(r) \triangleq y_H(rh)\}_{r=n-L}^{n-1}$ and $\{u_d(r) \triangleq u_H(rh)\}_{r=n-L}^{n-1}$ of length L, at the instant $t = nh$, where $n \geq L$.

Let

$$Y_L^n(e^{\mathrm{i}\omega_k}) \;=\; \sum_{m=0}^{L-1} y_d(m+n-L)e^{-\mathrm{i}\omega_k m} \tag{24}$$

and

$$U_L^n(e^{\mathrm{i}\omega_k}) \;=\; \sum_{m=0}^{L-1} u_d(m+n-L)e^{-\mathrm{i}\omega_k m} \tag{25}$$

where

$$\omega_k = \begin{cases} \frac{2\pi k}{L} & k = 0, 1, \ldots, \frac{L}{2} \\ \frac{2\pi(k-L)}{L} & k = \frac{L}{2}+1, \ldots, L-1, \end{cases} \tag{26}$$

be the Discrete Fourier transform (DFT) of the windowed data $\{y_d(r)\}_{r=n-L}^{N-1}$ and $\{u_d(r)\}_{r=k-L}^{n-1}$.

Let

$$E_L^n(e^{\mathrm{i}\omega_k}, \theta) \;\triangleq\; Y_L^n(e^{\mathrm{i}\omega_k}) - \hat{Y}_L^n(e^{\mathrm{i}\omega_k}, \theta), \tag{27}$$

where

$$\hat{Y}_L^n(e^{\mathrm{i}\omega_k}, \theta) \;\triangleq\; G_S(e^{\mathrm{i}\omega_k}, \theta)U_L^n(e^{\mathrm{i}\omega_k}), \tag{28}$$

and

$$V_L^n(\theta) \;\triangleq\; \sum_{k=0}^{L-1} \mid E_L^n(e^{\mathrm{i}\omega_k}, \theta) \mid^2 . \tag{29}$$

The FD-R algorithm is defined by the following recursion

$$\hat{\theta}(n) \;=\; \hat{\theta}(n-1) - \frac{1}{n-L+1}[V_L^{n\,''}(\hat{\theta}(n-1))]^{-1}V_L^{n\,'}(\hat{\theta}(n-1)) \tag{30}$$

where $V_L^{n\,'}(\theta)$ and $V_L^{n\,''}(\theta)$ are the first and second derivatives of $V_L^n(\theta)$, (29), with respect to θ. See [5] for details on computing $V_L^{n\,'}(\theta)$ and $V_L^{n\,''}(\theta)$ and implementing the recursion (30).

It [5], we have shown that the recursion (30) approximately minimizes the cost function

$$W_L^N(\theta) \;\triangleq\; \frac{1}{N-L+1}\sum_{n=L}^{N} V_L^n(\theta), \tag{31}$$

at the instant $t = Nh$.

4.2 Windowed Frequency Domain Recursive Algorithm (WFD-R)

The WFD-R algorithm is defined by the recursion

$$\tilde{\theta}(n) \quad = \quad \tilde{\theta}(n-1) - [V_L^{n\,''}(\tilde{\theta}(n-1))]^{-1}[V_L^{n\,'}(\tilde{\theta}(n-1))]. \tag{32}$$

where $V_L^{n\,'}(\theta)$ and $V_L^{n\,''}(\theta)$ are the derivatives of $V_L^n(\theta)$, (29), with respect to θ. Details on implementing the WFD-R algorithm can be found in [5].

In [5], we have presented the derivation of the WFD-R algorithm, wherein we have shown that

$$\tilde{\theta}(n) \approx \arg\min_{\theta} V_L^n(\theta). \tag{33}$$

5 Convergence Analysis

In this section, we analyse the convergence properties of the FD-R algorithm, see (30). Convergence of the WFD-R algorithm, (32), will be discussed in brief in Section 6. Here, we will show that, under certain conditions the minimizer of the cost function (31), *i.e.,*

$$\theta(N) \quad = \quad \arg\min_{\theta} W_L^N(\theta), \tag{34}$$

can be made arbitrarily close to θ_0 by choosing large values of N and L. To this end, we will first show that the limits

$$W_L(\theta) \quad \triangleq \quad \lim_{N\to\infty} W_L^N(\theta) \tag{35}$$

and

$$W(\theta) \quad \triangleq \quad \lim_{L\to\infty} W_L(\theta) \tag{36}$$

exist and their respective convergences are uniform in θ. We then show that $W(\theta)$, (36), which by construction is positive, and is equal to zero, *i.e.,*

$$W(\theta) = 0, \tag{37}$$

iff $\theta = \theta_0$. To infer the connection between (35), (36) and (37) and the claim that $\theta(N) \approx \theta_0$ for large values of N and L, note that uniform convergence of the limits (35) and (36) implies

$$\arg\min_{\theta} W_L^N(\theta) \longrightarrow \arg\min_{\theta} W_L(\theta) \tag{38}$$

as $N \to \infty$ and

$$\arg\min_{\theta} W_L(\theta) \longrightarrow \arg\min_{\theta} W(\theta) \tag{39}$$

as $L \to \infty$, see [12]. Hence, if it can be shown that the minimizer of $W(\theta)$ is θ_0, then it is fairly straightforward to see that the minimizer of $W_L^N(\theta)$, which is $\theta(N)$, can be made arbitrarily close to θ_0 by choosing large N and L.

5.1 Assumptions and Properties

In this subsection, we introduce three assumptions, (A1), (A2) and (A3), which are crucial for proving (35), (36) and (37). Further, we also discuss certain key properties of the sampled system, which are important for our proof.

A1. The FD-R estimates $\hat{\theta}(n)$, (30), and the WFD-R estimates $\tilde{\theta}(n)$, (32), belong to a compact set $\mathcal{D}$, such that $\theta_0 \in \mathcal{D}$, and $\mathcal{D}$ is contained in the positive quadrant of $\mathbb{R}^2$.

A2. The inputs $\{u_d(n)\}_{n=0}^{\infty}$ are bounded and satisfy the ergodicity condition,

$$\lim_{N\to\infty} \frac{1}{N} \sum_{n=0}^{N-1} u_d(n)u_d(n+m) \;\triangleq\; r(m) \;\; m \;\geq\; 0 \tag{40}$$

$\{r(m)\}_{m=0}^{\infty}$ is a bounded finite sequence of real numbers.

A3. The covariance sequence $\{r(m)\}_{m=0}^{\infty}$ is finite, *i.e.,* there exists an integer $N_1 > 0$, such that

$$r(m) \;\triangleq\; 0, \;\; m \;\geq\; N_1. \tag{41}$$

Assumption (A1) ensures the stability of the model output. A standard practice to ensure that $\hat{\theta}(n)$ and $\tilde{\theta}(n)$ does not violate (A1) is to incorporate a projection mechanism in the algorithms, which would push the iterates back in to the parameter set $\mathcal{D}$. Assumption (A2) is commonly used in many estimation problems in signal processing. See [16] for conditions under which (40) holds. Assumption (A3) is introduced primarily for technical ease in the analysis. As N_1 can be large (but finite) a wide class of inputs is indeed covered by the assumptions (A2) and (A3).

Since the true system model with the transfer-function $G(s,\theta)$, see (7) and (8), is *bounded input bounded output* (BIBO) stable for all $\theta \in \mathcal{D}$, the sampled output corresponding to a bounded input is always bounded. Therefore the sampled model

$$Y_S(e^{\mathrm{i}\omega},\theta) \;\triangleq\; G_S(e^{\mathrm{i}\omega},\theta)U_S(e^{\mathrm{i}\omega}), \tag{42}$$

where $G_S(e^{\mathrm{i}\omega},\theta)$ is as in (23) with θ_0 replaced by θ, is also BIBO stable for all $\theta \in \mathcal{D}$, see also Figure 1. More important than the BIBO stability of (42) is the following consequence of it, which will often be used in our proof. Note that by definition the sampled model (42) is a discrete time convolution system in the time domain. Hence due to BIBO stability of (42), the inverse discrete Fourier transform (IDFT) sequence

$$g_{H_d}(n,\theta) \;\triangleq\; \frac{1}{2\pi}\int_{-\pi}^{\pi} G_S(e^{\mathrm{i}\omega},\theta)e^{\mathrm{i}\omega n}d\omega, \;\; n = 0,1,2,\ldots, \tag{43}$$

of $G_S(e^{\mathrm{i}\omega},\theta)$, is absolutely summable, *i.e.*,

$$\sum_{n=0}^{\infty} \mid g_{H_d}(n,\theta) \mid < \;\infty, \;\; \forall\theta \in \mathcal{D} \tag{44}$$

see page 103 of [1] for a proof.

To further examine $g_{H_d}(n,\theta)$ we have made some numerical illustrations. As $g_{H_d}(n,\theta)$ is a two dimensional vector,

$$g_{H_d}(n,\theta) \;\triangleq\; [g_{H_d,1}(n,\theta)\;,\; g_{H_d,2}(n,\theta)]\,, \tag{45}$$

we have plotted the normalized components

$$\bar{g}_{H_d,i}(n,\theta) \;\triangleq\; \frac{g_{H_d,i}(n,\theta)}{\max_n \mid g_{H_d,i}(n,\theta) \mid}, \;\; i = 1,2 \tag{46}$$

of $g_{H_d}(n,\theta)$ in Figures 5 and 6 for $\theta = (2 + 0.5 \times k, 1)$, $k = 0,1,2,\ldots,10$, with the sampling rate $h = 0.01$. Note that we have only varied the α of the parameter θ and kept κ as a constant equal to one. Using the expression derived for $G_S(e^{\mathrm{i}\omega},\theta)$, (23), in (43), see also (8) and (17), it can be inferred that κ only scales $\bar{g}_{H_d,1}(n,\theta)$ by a factor $\frac{1}{\kappa}$, and has no effect on $\bar{g}_{H_d,2}(n,\theta)$. Hence variations in κ do not have any effect on the rate of convergence of $\bar{g}_{H_d,1}(n,\theta)$ and $\bar{g}_{H_d,2}(n,\theta)$. Figures 5 and 6 suggest that, for the chosen values of θ and h,

$$g_{H_d,1}(n,\theta) \;\sim\; O\left(\frac{1}{n^2}\right) \tag{47}$$

and

$$g_{H_d,2}(n,\theta) \;\sim\; O\left(\frac{1}{n^\delta}\right) \;\; \delta \;>\; 2 \tag{48}$$

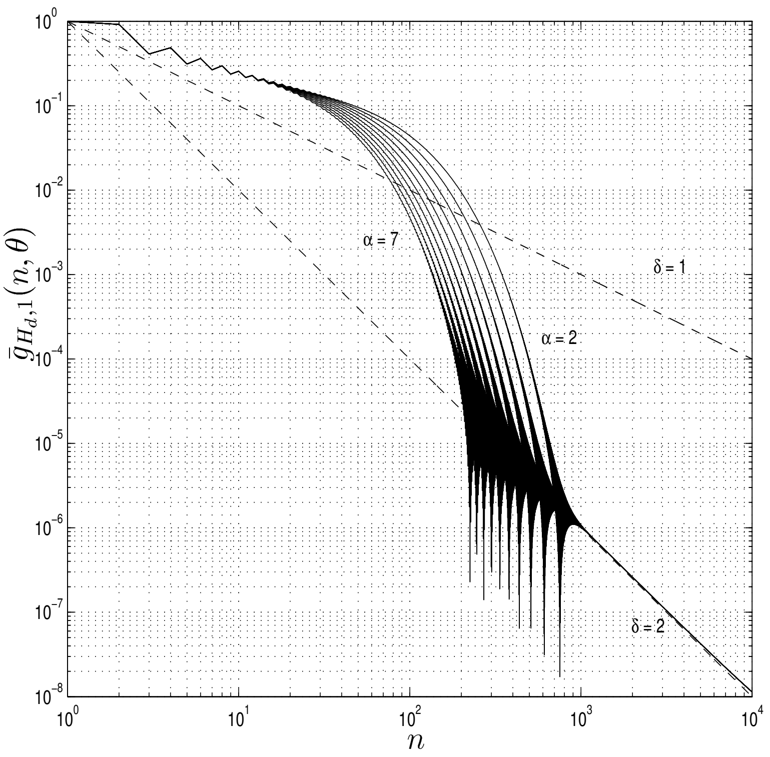

Figure 5: Plot of $g_{H_d,1}(n, \theta)$ for $\theta = (2 + 0.5 \times k, 1)$, where $k = 0, 1, 2, \ldots, 10$, with the sampling rate $h = 0.01$. The dotted lines in the plot denotes $\frac{1}{n^\delta}$, for $\delta = 1, 2$. Note from the figure that the value of δ corresponding to $g_{H_d,1}(n, \theta)$, is close to 2.

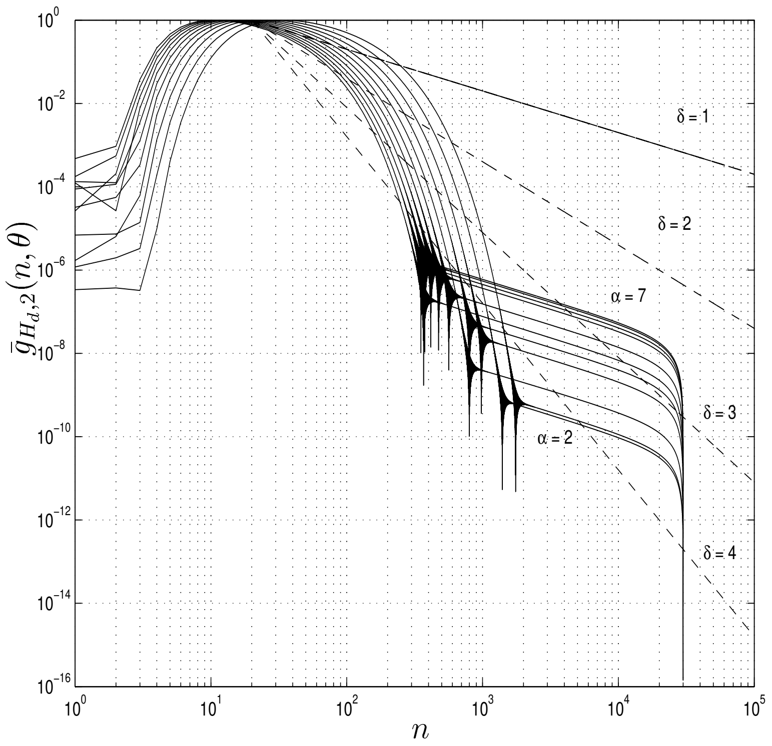

Figure 6: Plot of $g_{H_d,2}(n,\theta)$ for $\theta = (2 + 0.5 \times k, 1)$, $k = 0, 1, 2, \ldots, 10$, with the sampling rate $h = 0.01$. The dotted lines in the plot denotes $\frac{1}{n^\delta}$, for $\delta = 1, 2, 3, 4$. From the figure the value of δ for $g_{H_d,2}(n,\theta)$ larger than 2.

5.2 Detailed Analysis

We now move on to establish the existence and the uniform convergence of the limits (35) and (36), and also show that the minimizer of $W(\theta)$, (36), is at $\theta = \theta_0$, (37). In the analysis to be presented here, we will introduce some approximations which would make the expressions involved elegant and technically easier to present. One can still prove (35), (36) and (37) without introducing these approximations, but at the expense of involving cumbersome and long expressions.

Here, though the cost functions $W(\theta)$, $W_L(\theta)$, $W_L^N(\theta)$ and $V_L^n(\theta)$ are all defined in the frequency domain, we transform them to the time domain and perform the convergence analysis therein. Using Parseval's relation, see [9], on (29) we get

$$V_L^n(\theta) \quad = \quad \frac{1}{L}\sum_{m=0}^{L-1}[\varepsilon_L^n(n-L+m,\theta)]^2, \tag{49}$$

where

$$\varepsilon_L^n(n-L+m,\theta) \quad \triangleq \quad y_d(n-L+m) - \hat{y}_L^n(n-L+m,\theta), \tag{50}$$

and

$$\hat{y}_L^n(n-L+m,\theta) \quad \triangleq \quad \frac{1}{L}\sum_{k=0}^{L-1}\hat{Y}(e^{\mathrm{i}\omega_k})e^{\mathrm{i}\omega_k m}. \tag{51}$$

Therefore to analyse $V_L^n(\theta)$ one has to characterise (50). Consider the second term $\hat{y}_L^n(n-L+m,\theta)$ in the right hand side (RHS) of (50). Using (28) in (51), we get

$$\hat{y}_L^n(n-L+m,\theta) \quad = \quad \frac{1}{L}\sum_{k=0}^{L-1}G_S(e^{\mathrm{i}\omega_k},\theta)U_L^n(e^{\mathrm{i}\omega_k})e^{\mathrm{i}\omega_k m}. \tag{52}$$

Further using (25) for $U_L^n(e^{\mathrm{i}\omega_k})$, (43) can be rewritten as

$$\begin{aligned}
\hat{y}_L^n(n-L+m,\theta) \quad &= \quad \frac{1}{L}\sum_{k=0}^{L-1}G_S(e^{\mathrm{i}\omega_k},\theta)\left\{\sum_{r=0}^{L-1}u_d(n-L+r)e^{-\mathrm{i}\omega_k r}\right\}e^{\mathrm{i}\omega_k m} \\
&= \quad \sum_{r=0}^{L-1}\left\{\frac{1}{L}\sum_{k=0}^{L-1}G_S(e^{\mathrm{i}\omega_k},\theta)e^{\mathrm{i}\omega_k(m-r)}\right\}u_d(n-L+r) \\
&= \quad \sum_{r=0}^{L-1}\hat{g}_{H_d}(m-r,\theta)u_d(n-L+r),
\end{aligned} \tag{53}$$

where

$$\hat{g}_{H_d}(m,\theta) \triangleq \frac{1}{L}\sum_{k=0}^{L-1} G_S(e^{\mathrm{i}\omega_k},\theta)e^{\mathrm{i}\omega_k m}. \tag{54}$$

As (54) is periodic with period L, (53) is well defined for all $m = 0, 1, \ldots, L-1$.

Note that (54) is an L point inverse discrete Fourier transform (IDFT) of $G_S(e^{\mathrm{i}\omega},\theta)$, sampled at the frequency points $\{\omega_k\}_{k=0}^{L-1}$. Since $\{g_{H_d}(m,\theta)\}_{m=0}^{\infty}$ is the IDFT sequence of $G_S(e^{\mathrm{i}\omega},\theta)$, see (43), we have

$$\hat{g}_{H_d}(m,\theta) \;=\; \sum_{r=0}^{\infty} g_{H_d}(m+rL,\theta), \quad m = 0, 1, \ldots, L-1, \tag{55}$$

and a periodic extension of (55), with period L, for all other values of the index m, see pages 528 – 529 of [9] for a proof. In Figure 7, we have given a pictorial description of

$$\begin{aligned} \hat{g}_{H_d}(m,\theta) &= \sum_{r=0}^{\infty} g_{H_d}(m+rL,\theta) \\ &= g_{H_d}(m,\theta) + \sum_{r=1}^{\infty} g_{H_d}(m+rL,\theta) \end{aligned} \tag{56}$$

for $m = 0, 1, 2, \ldots, L-1$ and its periodic extension for all other values m.

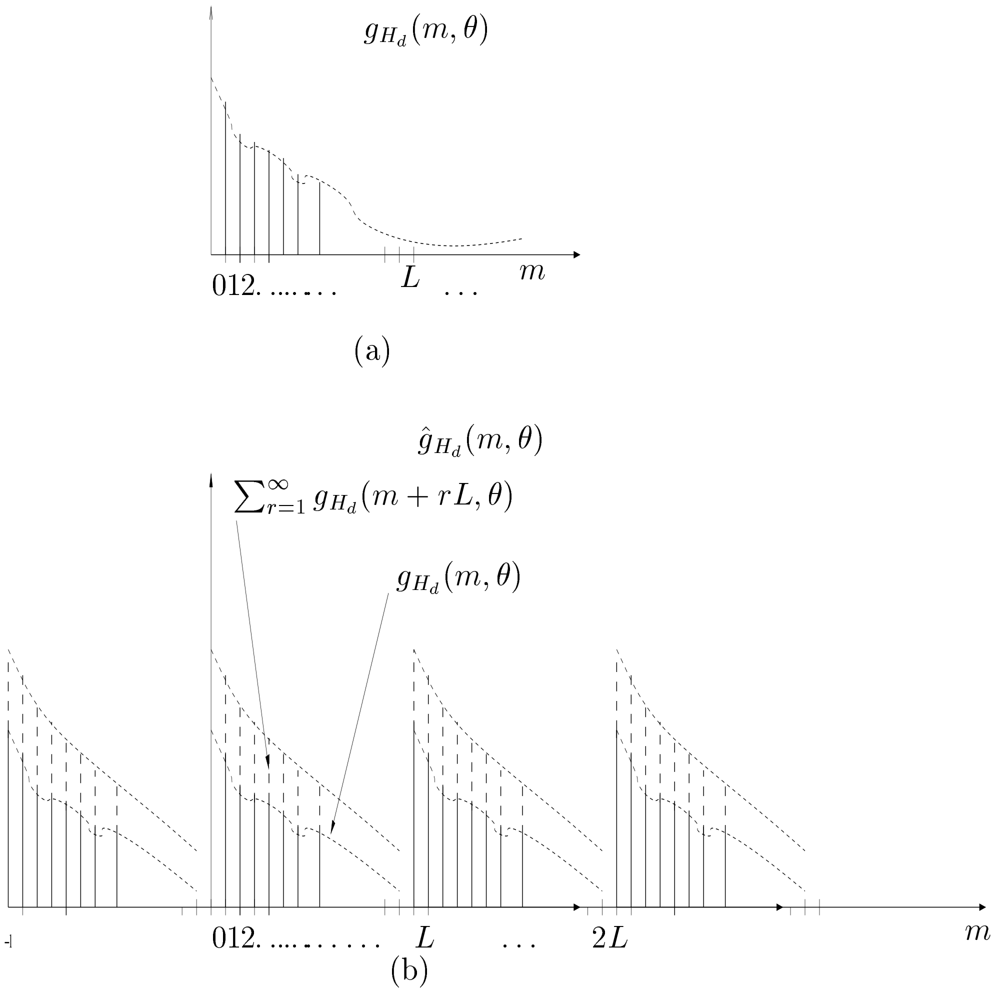

Figure 7: (a) describes the discrete sequence $\{g_{H_d}(m,\theta)\}_{m=0}^{\infty}$. (b) describes the corresponding periodic sequence $\{\hat{g}_{H_d}(m,\theta)\}_{m=0}^{L-1}$, see (55).

Note from Figure 7 that, the periodic sequence $\{\hat{g}_{H_d}(m,\theta)\}_{m=0}^{\infty}$ is effectively a sequence of shifted replicas of $\{g_{H_d}(m,\theta)+\sum_{r=1}^{\infty} g_{H_d}(m+rL,\theta)\}_{m=0}^{L-1}$.

If $\{g_{H_d}(m,\theta)\}_{m=0}^{\infty}$ were to be a finite length sequence of length L, *i.e.* $g_{H_d}(m,\theta) = 0$ for all $m = L, L+1, \ldots$, then (56) would imply that

$$\hat{g}_{H_d}(m,\theta) \quad = \quad g_{H_d}(m,\theta), \;\; \text{for} \;\; m = 0,1,\ldots,L-1 \tag{57}$$

and a periodic extension of (57) for all other values of m, see also Figure 8 for a pictorial description of (57) with its periodic extension. Note from Figure 8

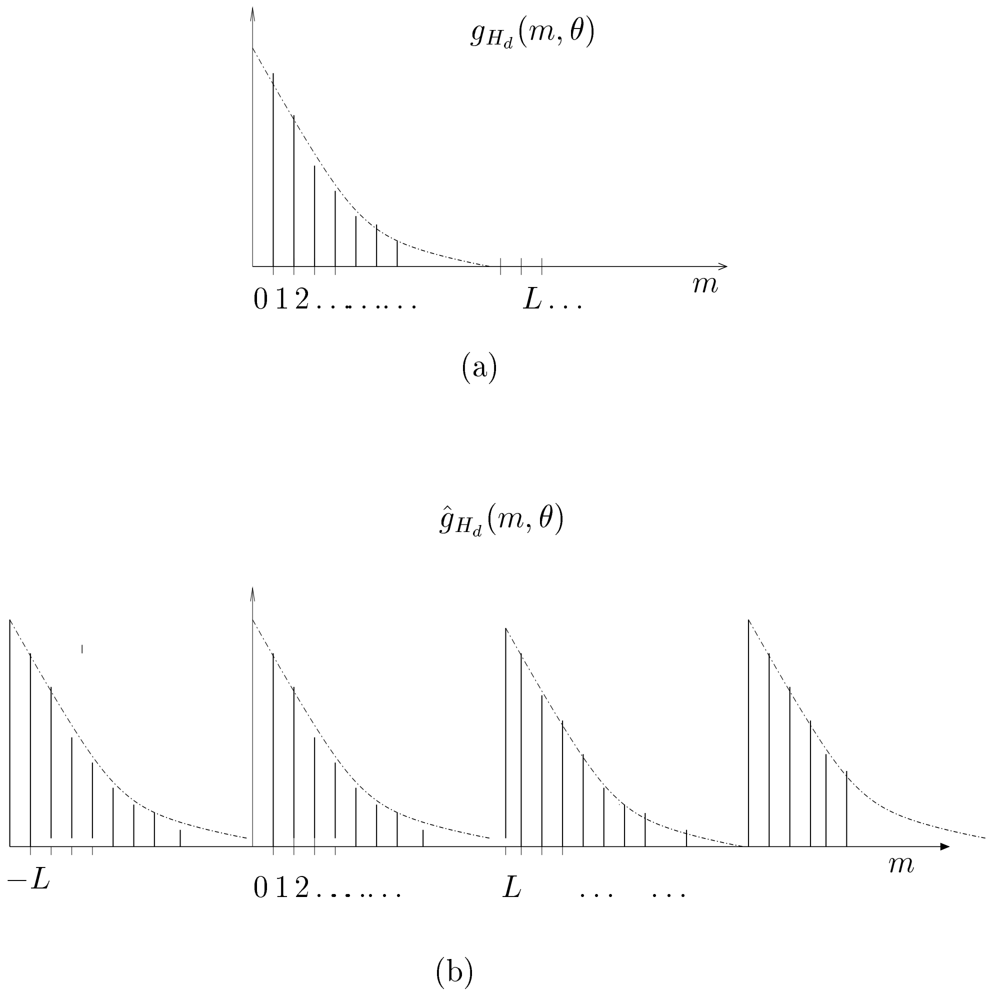

Figure 8: (a) describes a finite length discrete sequence $\{g_{H_d}(m,\theta)\}_{m=0}^{L-1}$ of length L. (b) describes the corresponding periodic sequence $\{\hat{g}_{H_d}(m,\theta)\}_{m=0}^{\infty}$, see (57).

that the periodic sequence $\{\hat{g}_{H_d}(m,\theta)\}_{m=0}^{\infty}$ is effectively a sequence of shifted replicas of $\{g_{H_d}(m,\theta)\}_{m=0}^{L-1}$.

In the current context the IDFT sequence $\{g_{H_d}(m,\theta)\}_{m=0}^{\infty}$ is not finite but only absolutely summable, see (44). Nevertheless, since $\{g_{H_d}(m,\theta)\}_{m=0}^{\infty}$

is absolutely summable, for large values of L the factor

$$\sum_{r=1}^{\infty} g_{H_d}(m+rL,\theta), \tag{58}$$

forms the tail of a convergent sum. Hence by choosing a large L, we neglect the sum (58) in (56) and obtain the approximation

$$\hat{g}_{H_d}(m,\theta) \approx g_{H_d}(m,\theta), \quad m=0,1,\ldots,L-1, \tag{59}$$

and a periodic extension of (59) for all other values of m, see also Figure 8. Using (59) in (53), we get

$$\begin{aligned}\hat{y}_L^n(n-L+m,\theta) \approx & \left\{ \sum_{r=0}^{m} g_{H_d}(m-r,\theta)u_d(n-L+r) \right. \\ & \left. + \sum_{r=m+1}^{L-1} g_{H_d}(m-r+L,\theta)u_d(n-L+r) \right\}, \end{aligned} \tag{60}$$

for all $m=0,1,2,\ldots,L-1$. To ease the notations, we define

$$\boldsymbol{g}(\theta) \triangleq \begin{bmatrix} g_{H_d}(0,\theta) & g_{H_d}(1,\theta) & \ldots & g_{H_d}(L-1,\theta) \end{bmatrix}^{\top} \tag{61}$$

$$\boldsymbol{u}_{n,L}^{(m)} \triangleq \begin{bmatrix} u_d(n-L+m) & u_d(n-L+m-1) & \ldots & u_d(n-L) \end{bmatrix}^{\top} \tag{62}$$

and

$$\boldsymbol{\phi}_{n,L}^{(m)} \triangleq \begin{bmatrix} u_d(n-1) & u_d(n-2) & \ldots & u_d(n-L+m+1) \end{bmatrix}^{\top} \tag{63}$$

where $\boldsymbol{g}(\theta)$ is of dimension $L \times 1$, $\boldsymbol{u}_{n,L}^{(m)}$ is of dimension $(m+1)$ and $\boldsymbol{\phi}_{n,L}^{(m)}$ is of dimension $L-(m+1)$. Further, from now on $\boldsymbol{o}_{l\times k}$ would denote an $l \times k$ matrix with zeros as its elements. Using the above defined notations (61) - (63) and $\boldsymbol{o}_{l\times k}$, (60) can be written in a vectorized form

$$\hat{y}_L^N(N-L+m,\theta) \approx \boldsymbol{g}^{\top}(\theta) \begin{bmatrix} \boldsymbol{u}_{n,L}^{(m)} \\ \boldsymbol{o}_{(L-(m+1))\times 1} \end{bmatrix} + \boldsymbol{g}^{\top}(\theta) \begin{bmatrix} \boldsymbol{o}_{(m+1)\times 1} \\ \boldsymbol{\phi}_{n,L}^{(m)} \end{bmatrix} \tag{64}$$

Now consider $y_d(n-L+m)$, which is $y_H(t)$ sampled at the instants $t = (n-L+m)h$. From (22), we can infer that $y_d(n-L+m)$ can be considered as a convolution of the IDFT of $G_S(e^{\mathrm{i}\omega},\theta_0)$, see (43), and the input sequence $\{u_d(n)\}_{n=0}^{\infty}$. Hence

$$y_d(n-L+m) = \sum_{r=0}^{n-L+m} g_{H_d}(n-L+m-r,\theta_0)u_d(r). \tag{65}$$

We split the sum in (65) into three parts and rewrite the RHS of (65) as

$$
\begin{aligned}
y_d(n-L+m) \;=\; & \sum_{r=0}^{n-2L+m} g_{H_d}(n-L+m-r,\theta_0)u_d(r) \\
& + \sum_{r=n-2L+m+1}^{n-L-1} g_{H_d}(n-L+m-r,\theta_0)u_d(r) \\
& + \sum_{r=n-L}^{n-L+m} g_{H_d}(n-L+m-r,\theta_0)u_d(r). \qquad (66)
\end{aligned}
$$

Since the inputs $\{u_d(n)\}_{n=0}^{\infty}$ are bounded for all n and $\{g_{H_d}(n,\theta)\}_{n=0}^{\infty}$ is an absolutely summable sequence, see (44), as before, by taking L to be very large one can neglect the first sum in the RHS of (66), which corresponds to the initial transients, and approximate $y_d(n-L+m)$ by

$$
\begin{aligned}
y_d(n-L+m) \;\approx\; & \sum_{r=n-2L+m+1}^{n-L-1} g_{H_d}(n-L+m-r,\theta_0)u_d(r) \\
& + \sum_{r=n-L}^{n-L+m} g_{H_d}(n-L+m-r,\theta_0)u_d(r). \qquad (67)
\end{aligned}
$$

To make (67) compatible with (64), we first change the index of second sum in the RHS of (67) from r to $r^{'} = r-n+L$, which leads to

$$
\begin{aligned}
y_d(n-L+m) \;\approx\; & \sum_{r=n-2L+m+1}^{n-L-1} g_{H_d}(n-L+m-r,\theta_0)u_d(r) \\
& + \sum_{r^{'}=0}^{m} g_{H_d}(m-r^{'},\theta_0)u_d(n-L+r^{'}). \qquad (68)
\end{aligned}
$$

Further, setting

$$
\begin{aligned}
& \boldsymbol{\psi}_{n,L}^{(m)} \triangleq \\
& \left[\begin{array}{cccc} u_d(n-L-1) & u_d(n-L-2) & \ldots & u_d(n-2L+(m+1)) \end{array}\right]^{\top}, (69)
\end{aligned}
$$

which is of dimension $L-(m+1)$, and using (61) (62), and $\boldsymbol{o}_{l\times k}$, equation (68) can be re-written in the vector form

$$
y_d(n-L+m) \;\approx\; \boldsymbol{g}^{\top}(\theta_0)\begin{bmatrix} \boldsymbol{o}_{(m+1)\times 1} \\ \boldsymbol{\psi}_{n,L}^{(m)} \end{bmatrix} + \boldsymbol{g}^{\top}(\theta_0)\begin{bmatrix} \boldsymbol{u}_{n,L}^{(m)} \\ \boldsymbol{o}_{(L-(m+1))\times 1} \end{bmatrix}. (70)
$$

Hence, using (64) and (70) in (50), we have

$$\begin{aligned}
\varepsilon_L^n(n-L+m,\theta) &= y_d(n-L+m) - \hat{y}_L^n(n-L+m,\theta) \\
&\approx \boldsymbol{g}^\top(\theta_0)\left[\begin{array}{l} \boldsymbol{o}_{(m+1)\times 1} \\ \boldsymbol{\psi}_{n,L}^{(m)} \end{array}\right] \\
&\quad +\tilde{\boldsymbol{g}}(\theta)^\top \left[\begin{array}{l} \boldsymbol{u}_{n,L}^{(m)} \\ \boldsymbol{o}_{(L-(m+1))\times 1} \end{array}\right] \\
&\quad -\boldsymbol{g}^\top(\theta)\left[\begin{array}{l} \boldsymbol{o}_{(m+1)\times 1} \\ \boldsymbol{\phi}_{n,L}^{(m)} \end{array}\right], \qquad (71)
\end{aligned}$$

where

$$\tilde{\boldsymbol{g}}(\theta) \triangleq \boldsymbol{g}(\theta_0) - \boldsymbol{g}(\theta). \qquad (72)$$

Having derived an expression $\varepsilon_L^n(n-L+m,\theta)$, we now move on to prove (35), (36) and (37). Note from (31) and (49) that

$$\begin{aligned}
W_L^N(\theta) &= \frac{1}{N-L+1}\sum_{n=L}^{N} V_L^n(\theta) \\
&= \frac{1}{N-L+1}\sum_{n=L}^{N}\left\{\frac{1}{L}\sum_{m=0}^{L-1}[\varepsilon_L^n(n-L+m,\theta)]^2\right\} \\
&= \frac{1}{L}\sum_{m=0}^{L-1}\left\{\frac{1}{N-L+1}\sum_{n=L}^{N}[\varepsilon_L^n(n-L+m,\theta)]^2\right\}, \qquad (73)
\end{aligned}$$

To determine the limit of $W_L^N(\theta)$ as $N\to\infty$, consider a typical term,

$$\beta \triangleq \frac{1}{N-L+1}\sum_{n=L}^{N}[\varepsilon_L^n(n-L+m,\theta)]^2, \qquad (74)$$

in the finite outer sum of (73). Using (71) in (74) and expanding the square, we get

$$
\begin{aligned}
\beta \;=\; & \frac{1}{N-L+1}\left\{\sum_{n=L}^{N}\boldsymbol{g}^{\top}(\theta_0)\begin{bmatrix}\boldsymbol{o}_{(m+1)\times 1}\\ \boldsymbol{\psi}_{n,L}^{(m)}\end{bmatrix}\begin{bmatrix}\boldsymbol{o}_{1\times(m+1)} & \boldsymbol{\psi}_{n,L}^{(m)\top}\end{bmatrix}\boldsymbol{g}(\theta_0)\right.\\
& +\sum_{n=L}^{N}\tilde{\boldsymbol{g}}^{\top}(\theta)\begin{bmatrix}\boldsymbol{u}_{n,L}^{(m)}\\ \boldsymbol{o}_{(L-(m+1))\times 1}\end{bmatrix}\begin{bmatrix}\boldsymbol{u}_{n,L}^{(m)\top} & \boldsymbol{o}_{1\times(L-(m+1))}\end{bmatrix}\tilde{\boldsymbol{g}}(\theta)\\
& +\sum_{n=L}^{N}\boldsymbol{g}^{\top}(\theta)\begin{bmatrix}\boldsymbol{o}_{(m+1)\times 1}\\ \boldsymbol{\phi}_{n,L}^{(m)}\end{bmatrix}\begin{bmatrix}\boldsymbol{o}_{1\times(m+1)} & \boldsymbol{\phi}_{n,L}^{(m)\top}\end{bmatrix}\boldsymbol{g}(\theta)\\
& +2\sum_{n=L}^{N}\boldsymbol{g}^{\top}(\theta_0)\begin{bmatrix}\boldsymbol{o}_{(m+1)\times 1}\\ \boldsymbol{\psi}_{n,L}^{(m)}\end{bmatrix}\begin{bmatrix}\boldsymbol{u}_{n,L}^{(m)\top} & \boldsymbol{o}_{1\times(L-(m+1))}\end{bmatrix}\tilde{\boldsymbol{g}}(\theta)\\
& -2\sum_{n=L}^{N}\tilde{\boldsymbol{g}}^{\top}(\theta)\begin{bmatrix}\boldsymbol{u}_{n,L}^{(m)}\\ \boldsymbol{o}_{(L-(m+1))\times 1}\end{bmatrix}\begin{bmatrix}\boldsymbol{o}_{1\times(m+1)} & \boldsymbol{\phi}_{n,L}^{(m)\top}\end{bmatrix}\boldsymbol{g}(\theta)\\
& \left.-2\sum_{n=L}^{N}\boldsymbol{g}^{\top}(\theta_0)\begin{bmatrix}\boldsymbol{o}_{(m+1)\times 1}\\ \boldsymbol{\psi}_{n,L}^{(m)}\end{bmatrix}\begin{bmatrix}\boldsymbol{o}_{1\times(m+1)} & \boldsymbol{\phi}_{n,L}^{(m)\top}\end{bmatrix}\boldsymbol{g}(\theta)\right\}. \qquad (75)
\end{aligned}
$$

Now consider the first sum in (75). Note that

$$
\begin{aligned}
& \frac{1}{N-L+1}\sum_{n=L}^{N}\boldsymbol{g}^{\top}(\theta_0)\begin{bmatrix}\boldsymbol{o}_{(m+1)\times 1}\\ \boldsymbol{\psi}_{n,L}^{(m)}\end{bmatrix}\begin{bmatrix}\boldsymbol{o}_{1\times(m+1)\times 1} & \boldsymbol{\psi}_{n,L}^{(m)\top}\end{bmatrix}\boldsymbol{g}(\theta_0)\\
= \; & \frac{\boldsymbol{g}^{\top}(\theta_0)}{N-L+1}\sum_{n=L}^{N}\begin{bmatrix}\boldsymbol{o}_{(m+1)\times(m+1)} & \boldsymbol{o}_{(m+1)\times(L-(m+1))}\\ \boldsymbol{o}_{(L-(m+1))\times(m+1)} & \boldsymbol{\psi}_{n,L}^{(m)}\boldsymbol{\psi}_{n,L}^{(m)\top}\end{bmatrix}\boldsymbol{g}(\theta_0). \qquad (76)
\end{aligned}
$$

Using the assumption (A2) and taking the limits, we get

$$
\begin{aligned}
& \lim_{N\to\infty}\frac{\boldsymbol{g}^{\top}(\theta_0)}{N-L+1}\sum_{n=L}^{N}\begin{bmatrix}\boldsymbol{o}_{(m+1)\times(m+1)} & \boldsymbol{o}_{(m+1)\times(L-(m+1))}\\ \boldsymbol{o}_{(L-(m+1))\times(m+1)} & \boldsymbol{\psi}_{n,L}^{(m)}\boldsymbol{\psi}_{n,L}^{(m)\top}\end{bmatrix}\boldsymbol{g}(\theta_0)\\
= \; & \boldsymbol{g}^{\top}(\theta_0)\begin{bmatrix}\boldsymbol{o}_{(m+1)\times(m+1)} & \boldsymbol{o}_{(m+1)\times(L-(m+1))}\\ \boldsymbol{o}_{(L-(m+1))\times(m+1)} & \boldsymbol{R}_{\psi\psi}(m)\end{bmatrix}\boldsymbol{g}(\theta_0), \qquad (77)
\end{aligned}
$$

where

$$
\begin{aligned}
& \boldsymbol{R}_{\psi\psi}(m) \triangleq\\
& \begin{bmatrix}
r(0) & r(1) & \dots & r(L-(m+2))\\
r(1) & r(0) & \dots & r(L-(m+3))\\
\vdots & \vdots & \ddots & \vdots\\
r(L-(m+2)) & r(L-(m+3)) & \dots & r(0)
\end{bmatrix}. \qquad (78)
\end{aligned}
$$

Similarly, consider the second sum in (75). As in (76), we have

$$
\begin{aligned}
&\frac{1}{N-L+1}\sum_{n=L}^{N}\tilde{\boldsymbol{g}}(\theta)^\top \begin{bmatrix} \boldsymbol{u}_{n,L}^{(m)} \\ \boldsymbol{o}_{(L-(m+1))\times 1} \end{bmatrix} \begin{bmatrix} \boldsymbol{u}_{n,L}^{(m)} & \boldsymbol{o}_{1\times(L-(m+1))} \end{bmatrix} \tilde{\boldsymbol{g}}(\theta) \\
= \;& \frac{\tilde{\boldsymbol{g}}(\theta)^\top}{N-L+1}\sum_{n=L}^{N} \begin{bmatrix} \boldsymbol{u}_{n,L}^{(m)}\boldsymbol{u}_{n,L}^{(m)\top} & \boldsymbol{o}_{(m+1)\times(L-(m+1))} \\ \boldsymbol{o}_{(L-(m+1))\times(m+1)} & \boldsymbol{o}_{(L-(m+1))\times(L-(m+1))} \end{bmatrix} \tilde{\boldsymbol{g}}(\theta). \quad (79)
\end{aligned}
$$

As before, using the assumption (A2) and taking limits, we get

$$
\begin{aligned}
&\lim_{N\to\infty}\frac{\tilde{\boldsymbol{g}}(\theta)^\top}{N-L+1}\sum_{n=L}^{N} \begin{bmatrix} \boldsymbol{u}_{n,L}^{(m)}\boldsymbol{u}_{n,L}^{(m)\top} & \boldsymbol{o}_{(m+1)\times(L-(m+1))} \\ \boldsymbol{o}_{(L-(m+1))\times(m+1)} & \boldsymbol{o}_{(L-(m+1))\times(L-(m+1))} \end{bmatrix} \tilde{\boldsymbol{g}}(\theta) \\
= \;& \tilde{\boldsymbol{g}}(\theta)^\top \begin{bmatrix} \boldsymbol{R}_{uu}(m) & \boldsymbol{o}_{(m+1)\times(L-(m+1))} \\ \boldsymbol{o}_{(L-(m+1))\times(m+1)} & \boldsymbol{o}_{(m+1)\times(m+1)} \end{bmatrix} \tilde{\boldsymbol{g}}(\theta)^\top, \qquad (80)
\end{aligned}
$$

where

$$
\boldsymbol{R}_{uu}(m) \triangleq \begin{bmatrix} r(0) & r(1) & \dots & r(m) \\ r(1) & r(0) & \dots & r(m-1) \\ \vdots & \vdots & \ddots & \vdots \\ r(m) & r(m-1) & \dots & r(0) \end{bmatrix}. \qquad (81)
$$

In (80), even though the convergence is established using Assumption (A2), this assumption does not directly imply that the convergence (80) is uniform in θ for all $\theta \in \mathcal{D}$, where $\mathcal{D}$ is as mentioned in (A1). In the appendix, we have shown that the convergence (80) is indeed uniform in θ for all $\theta \in \mathcal{D}$. Note that, the issue of uniform convergence does not arise in the case of (77), as it only involves θ_0 and not all $\theta \in \mathcal{D}$.

As done above, one can show that the other sums of (75) also converge uniformly in θ, for all $\theta \in \mathcal{D}$, to the following asymptotic matrices

$$
\begin{aligned}
&\lim_{N\to\infty}\frac{\boldsymbol{g}^\top(\theta)}{N-L+1}\sum_{n=L}^{N} \begin{bmatrix} \boldsymbol{o}_{(m+1)\times 1} \\ \boldsymbol{\phi}_{n,L}^{(m)} \end{bmatrix} \begin{bmatrix} \boldsymbol{o}_{1\times(m+1)} & \boldsymbol{\phi}_{n,L}^{(m)\top} \end{bmatrix} \boldsymbol{g}(\theta) \\
= \;& \boldsymbol{g}^\top(\theta) \begin{bmatrix} \boldsymbol{o}_{(m+1)\times(m+1)} & \boldsymbol{o}_{(m+1)\times(L-(m+1))} \\ \boldsymbol{o}_{(L-(m+1))\times(m+1)} & \boldsymbol{R}_{\phi\phi}(m) \end{bmatrix} \boldsymbol{g}(\theta), \qquad (82)
\end{aligned}
$$

where

$$
\boldsymbol{R}_{\phi\phi}(m) = \begin{bmatrix} r(0) & r(1) & \dots & r(L-(m+2)) \\ r(1) & r(0) & \dots & r(L-(m+3)) \\ \vdots & \vdots & \ddots & \vdots \\ r(L-(m+2)) & \dots & \dots & r(0) \end{bmatrix}. \qquad (83)
$$

$$\lim_{N\to\infty} \frac{\boldsymbol{g}^\top(\theta_0)}{N-L+1} \sum_{n=L}^{N} \begin{bmatrix} \boldsymbol{o}_{(m+1)\times 1} \\ \boldsymbol{\psi}_{n,L}^{(m)} \end{bmatrix} \begin{bmatrix} \boldsymbol{u}_{n,L}^{(m)\top} & \boldsymbol{o}_{1\times(L-(m+1))} \end{bmatrix} \tilde{\boldsymbol{g}}(\theta)$$

$$= \boldsymbol{g}^\top(\theta_0) \begin{bmatrix} \boldsymbol{o}_{(m+1)\times(m+1)} & \boldsymbol{o}_{(m+1)\times(L-(m+1))} \\ \boldsymbol{R}_{\psi u}(m) & \boldsymbol{o}_{(L-(m+1))\times(L-(m+1))} \end{bmatrix} \tilde{\boldsymbol{g}}(\theta)^\top, \tag{84}$$

where

$$\boldsymbol{R}_{\psi u}(m) = \begin{bmatrix} r(m+1) & r(m) & \dots & r(1) \\ r(m+2) & r(m+1) & \dots & r(2) \\ \vdots & \vdots & \ddots & \vdots \\ r(L-1) & r(L-2) & \dots & r(L-(m+1)) \end{bmatrix}. \tag{85}$$

$$\lim_{N\to\infty} \frac{\tilde{\boldsymbol{g}}^\top(\theta)}{N-L+1} \sum_{n=L}^{N} \begin{bmatrix} \boldsymbol{u}_{n,L}^{(m)} \\ \boldsymbol{o}_{(L-(m+1))\times 1} \end{bmatrix} \begin{bmatrix} \boldsymbol{o}_{1\times(m+1)} & \boldsymbol{\phi}_{n,L}^{(m)\top} \end{bmatrix} \boldsymbol{g}(\theta)$$

$$= \tilde{\boldsymbol{g}}^\top(\theta) \begin{bmatrix} \boldsymbol{o}_{(m+1)\times(m+1)} & \boldsymbol{R}_{u\phi} \\ \boldsymbol{o}_{(L-(m+1))\times(m+1)} & \boldsymbol{o}_{(L-(m+1))\times(L-(m+1))} \end{bmatrix} \boldsymbol{g}(\theta), \tag{86}$$

where

$$\boldsymbol{R}_{u\phi}(m) = \begin{bmatrix} r(L-(m+1)) & r(L-(m+2)) & \dots & r(1) \\ r(L-m) & r(L-(m+1)) & \dots & r(2) \\ \vdots & \vdots & \ddots & \vdots \\ r(L-1) & r(L-2) & \dots & r(m+1) \end{bmatrix}, \tag{87}$$

$$\lim_{N\to\infty} \frac{\boldsymbol{g}^\top(\theta_0)}{N-L+1} \sum_{n=L}^{N} \begin{bmatrix} \boldsymbol{o}_{(m+1)\times 1} \\ \boldsymbol{\psi}_{n,L}^{(m)} \end{bmatrix} \begin{bmatrix} \boldsymbol{o}_{1\times(m+1)} & \boldsymbol{\phi}_{n,L}^{(m)\top} \end{bmatrix} \boldsymbol{g}(\theta)$$

$$= \boldsymbol{g}^\top(\theta_0) \begin{bmatrix} \boldsymbol{o}_{(m+1)\times(m+1)} & \boldsymbol{o}_{(m+1)\times(L-(m+1))} \\ \boldsymbol{o}_{(L-(m+1))\times(m+1)} & \boldsymbol{R}_{\psi\phi}(m) \end{bmatrix} \boldsymbol{g}(\theta) \tag{88}$$

where

$$\boldsymbol{R}_{\psi\phi}(m) = \begin{bmatrix} r(L) & r(L-1) & \dots & r(m+2) \\ r(L+1) & r(L) & \dots & r(m+3) \\ \vdots & \vdots & \ddots & \vdots \\ r(2L-(m+2)) & r(2L-(m+3)) & \dots & r(L) \end{bmatrix}. \tag{89}$$

Hence, from (77), (80), (82), (84), (86) and (88), we have

$$\begin{aligned}
W_L(\theta) &\approx \frac{1}{L}\sum_{m=0}^{L-1}\left\{\boldsymbol{g}^\top(\theta_0)\begin{bmatrix} \boldsymbol{O}_{(m+1)\times(m+1)} & \boldsymbol{O}_{(m+1)\times(L-(m+1))} \\ \boldsymbol{O}_{(L-(m+1))\times(m+1)} & \boldsymbol{R}_{\psi\psi}(m)\end{bmatrix}\boldsymbol{g}(\theta_0)\right. \\
&+ \tilde{\boldsymbol{g}}(\theta)^\top\begin{bmatrix} \boldsymbol{R}_{uu}(m) & \boldsymbol{O}_{m+1\times(L-(m+1))} \\ \boldsymbol{O}_{(L-(m+1))\times(m+1)} & \boldsymbol{O}_{(L-(m+1))\times(L-(m+1))}\end{bmatrix}\tilde{\boldsymbol{g}}(\theta) \\
&+ \boldsymbol{g}^\top(\theta)\begin{bmatrix} \boldsymbol{O}_{(m+1)\times(m+1)} & \boldsymbol{O}_{(m+1)\times(L-(m+1))} \\ \boldsymbol{O}_{(L-(m+1))\times(m+1)} & \boldsymbol{R}_{\phi\phi}(m)\end{bmatrix}\boldsymbol{g}(\theta) \\
&+ 2\boldsymbol{g}^\top(\theta_0)\begin{bmatrix} \boldsymbol{O}_{(m+1)\times(m+1)} & \boldsymbol{O}_{(m+1)\times(L-(m+1))} \\ \boldsymbol{R}_{\psi u}(m) & \boldsymbol{O}_{(L-(m+1))\times(L-(m+1))}\end{bmatrix}\tilde{\boldsymbol{g}}(\theta) \\
&- 2\tilde{\boldsymbol{g}}^\top(\theta)\begin{bmatrix} \boldsymbol{O}_{(m+1)\times(m+1)} & \boldsymbol{R}_{u\phi}(m) \\ \boldsymbol{O}_{(L-(m+1))\times(m+1)} & \boldsymbol{O}_{(L-(m+1))\times(L-(m+1))}\end{bmatrix}\boldsymbol{g}(\theta) \\
&- \left. 2\boldsymbol{g}^\top(\theta_0)\begin{bmatrix} \boldsymbol{O}_{(m+1)\times(m+1)} & \boldsymbol{O}_{(m+1)\times(L-(m+1))} \\ \boldsymbol{O}_{(L-(m+1))\times(m+1)} & \mathbf{R}_{\psi\phi}(m)\end{bmatrix}\boldsymbol{g}(\theta)\right\} \\
&\triangleq \bar{W}_L^{(1,1)}(\theta_0) + \bar{W}_L^{(2,2)}(\theta) + \bar{W}_L^{(3,3)}(\theta) \\
&+ 2\bar{W}_L^{(1,2)}(\theta) - 2\bar{W}_L^{(2,3)}(\theta) - 2\bar{W}_L^{(1,3)}(\theta). \qquad (90)
\end{aligned}$$

Here, in (90), $W_L(\theta)$ is as defined in (35). Since the individual convergences (80), (82), (84), (86) and (88) are all uniform in θ, for all $\theta \in \mathcal{D}$, see subsection 8.1 in the appendix, the convergence involved in (90) is also uniform in θ for all $\theta \in \mathcal{D}$.

In the appendix, we have shown that the sums $\bar{W}_L^{(1,1)}(\theta_0)$, $\bar{W}_L^{(3,3)}(\theta)$, $\bar{W}_L^{(1,2)}(\theta)$, $\bar{W}_L^{(2,3)}(\theta)$ and $\bar{W}_L^{(1,3)}(\theta)$, in the RHS of (90) converge to zero as $L \to \infty$, for all $\theta \in \mathcal{D}$. In other words, we have shown that, see also (36),

$$\begin{aligned}
W(\theta) &= \lim_{L\to\infty} W_L(\theta) \\
&\approx \lim_{L\to\infty} \bar{W}_L^{(2,2)}(\theta) \triangleq \bar{W}^{(2,2)}(\theta), \qquad (91)
\end{aligned}$$

for all $\theta \in \mathcal{D}$.

As $\tilde{\boldsymbol{g}}(\theta_0) = 0$, it is evident that

$$\bar{W}^{(2,2)}(\theta_0) = 0. \qquad (92)$$

Further, it can also be shown that, see Lemma 4 in the appendix,

$$\bar{W}^{(2,2)}(\theta) > 0, \ \forall\, \theta \neq \theta_0, \ \ \theta \in \mathcal{D}. \qquad (93)$$

Alternatively, (92) and (93) imply that θ_0 is the unique minimizer of $\bar{W}^{(2,2)}(\theta)$, which approximately equals the limiting cost function $W(\theta)$.

6 Further Discussions and Extensions

In this section, we first discuss the possible weakening of Assumption (A3), which has been crucial for analyzing the convergence of the FD-R algorithm. We also discuss in brief the convergence of the WFD-R algorithm, (32). Finally, we interpret the results of the numerical experiments performed in [5], in the light of the above analysis.

Even though Assumption (A3) has seemingly been vital for the convergence analysis presented in section 5, it is more restrictive than necessary and does not encompass certain class of inputs which are often used by the practitioners of system identification. It can be inferred directly form (41) that all moving average (MA) processes, see [16], satisfy Assumption (A3) for some N_1. However, (A3) does not include auto-regressive moving average (ARMA) processes, which are often used as test inputs for identifying systems. In order, to include ARMA process, Assumption (A3) must be relaxed to the less stringent

A3'.

$$| \, r(m) \, | \quad \leq \quad r_0 \alpha^m \;\; \forall \, m = 0, 1, 2, \ldots, \tag{94}$$

for some $r_0 > 0$ and $0 < \alpha < 1$.

It is well known that for any given ARMA process there exists r_0 and α such that (19) holds. Technically this does not make any difference in the analysis, as in this case

$$\begin{aligned}
\| \, \boldsymbol{R}_{\psi\psi}(m) \, \|_1 &= \max_{1 \leq j \leq L-(m+1)} \sum_{i=1}^{L-(m+1)} | \, r(i-j) \, | \\
&\leq \max_{1 \leq j \leq L-(m+1)} \left[\sum_{i=1}^{L-(m+1)} r_0 \alpha^{|i-j|} \right] \\
&\leq r_0 \sum_{k=-\infty}^{\infty} \alpha^{|k|} \\
&\leq 2r_0 \sum_{k=0}^{\infty} \alpha^k \;=\; \frac{2r_0}{1-\alpha},
\end{aligned} \tag{95}$$

and hence is bounded.

From (33) and (49), we can infer that the iterates, $\tilde{\theta}(n)$, of the WFD-R algorithm approximately minimizes the cost function

$$V_L^n(\theta) \;=\; \frac{1}{L} \sum_{m=0}^{L-1} [\varepsilon_L^n(n-L+m, \theta)]^2, \tag{96}$$

where $\varepsilon_L^n(n-L+m,\theta)$ is as in (71). Using the expression (71) for $\varepsilon_L^n(n-L+m,\theta)$ in (96) and expanding squares, we get

$$
\begin{aligned}
V_L^n(\theta) \;=\; & \frac{1}{L}\sum_{m=0}^{L-1}\Bigg\{ \boldsymbol{g}^\top(\theta_0)\begin{bmatrix} \boldsymbol{o}_{(m+1)\times 1} \\ \boldsymbol{\psi}_{n,L}^{(m)} \end{bmatrix}\begin{bmatrix} \boldsymbol{o}_{1\times(m+1)} & \boldsymbol{\psi}_{n,L}^{(m)\top} \end{bmatrix}\boldsymbol{g}(\theta_0) \\
& +\tilde{\boldsymbol{g}}^\top(\theta)\begin{bmatrix} \boldsymbol{u}_{n,L}^{(m)} \\ \boldsymbol{o}_{(L-(m+1))\times 1} \end{bmatrix}\begin{bmatrix} \boldsymbol{u}_{n,L}^{(m)\top} & \boldsymbol{o}_{1\times(L-(m+1))} \end{bmatrix}\tilde{\boldsymbol{g}}(\theta) \\
& +\boldsymbol{g}^\top(\theta)\begin{bmatrix} \boldsymbol{o}_{(m+1)\times 1} \\ \boldsymbol{\phi}_{n,L}^{(m)} \end{bmatrix}\begin{bmatrix} \boldsymbol{o}_{1\times(m+1)} & \boldsymbol{\phi}_{n,L}^{(m)\top} \end{bmatrix}\boldsymbol{g}(\theta) \\
& +2\boldsymbol{g}^\top(\theta_0)\begin{bmatrix} \boldsymbol{o}_{(m+1)\times 1} \\ \boldsymbol{\psi}_{n,L}^{(m)} \end{bmatrix}\begin{bmatrix} \boldsymbol{u}_{n,L}^{(m)\top} & \boldsymbol{o}_{1\times(L-(m+1))} \end{bmatrix}\tilde{\boldsymbol{g}}(\theta) \\
& -2\tilde{\boldsymbol{g}}^\top(\theta)\begin{bmatrix} \boldsymbol{u}_{n,L}^{(m)} \\ \boldsymbol{o}_{(L-(m+1))\times 1} \end{bmatrix}\begin{bmatrix} \boldsymbol{o}_{1\times(m+1)} & \boldsymbol{\phi}_{n,L}^{(m)\top} \end{bmatrix}\boldsymbol{g}(\theta) \\
& -2\boldsymbol{g}^\top(\theta_0)\begin{bmatrix} \boldsymbol{o}_{(m+1)\times 1} \\ \boldsymbol{\psi}_{n,L}^{(m)} \end{bmatrix}\begin{bmatrix} \boldsymbol{o}_{1\times(m+1)} & \boldsymbol{\phi}_{n,L}^{(m)\top} \end{bmatrix}\boldsymbol{g}(\theta)\Bigg\} \\
\triangleq\; & \gamma_n.
\end{aligned} \tag{97}
$$

Note, from (73), that

$$W_L^N(\theta) \;=\; \frac{1}{N-L+1}\sum_{n=L}^{N}\gamma_n. \tag{98}$$

Unlike, $W_L^N(\theta)$, $V_L^n(\theta)$ does not involve any averaging with respect to the inputs. Therefore ergodicity assumptions of the type (A2), (A3) or (A3') are not permissible in the case of $V_L^n(\theta)$. Hence $V_L^n(\theta)$ does not have a limit as $n\to\infty$ and is also susceptible to the variations in the inputs for finite L. Nevertheless, if one assumes that the inputs are such that the matrices involving them in $V_L^n(\theta)$, (97), have their $\|\bullet\|_1$ norms uniformly bounded, then it is possible to show that the limit

$$\lim_{L\to\infty} V_L^n(\theta) \;\triangleq\; V(\theta) \tag{99}$$

exists and

$$V(\theta_0) = 0, \tag{100}$$

for any n. However, this assumption in turn requires the inputs to be absolutely summable, which is far too restrictive.

In [5] numerical experiments were performed using simulated input output data to test the effectiveness of the FD-R and the WFD-R algorithms. In the numerical experiments performed, the inputs were generated using known ARMA processes and the corresponding outputs were generated with the true parameter, θ_0, set to a known value. Precise details involving the generation of the inputs, computation of the outputs and the implementation of the FD-R and the WFD-R algorithm are presented in detail in [5]. The plots presented in [5] indicate that the sequence of estimates $\{\hat{\theta}(n)\}_{n=1}^{\infty}$ generated by the FD-R algorithm appeared to converge to a value close to θ_0 asymptotically, for all $L \geq 150$. Further, the plots also indicated that the asymptotic limit of the FD-R estimates approached θ_0 with increasing L. This is not surprising, as we know from the analysis done in Section 5 that the FD-R estimates approximately minimize the function $\bar{W}_L^{(2,2)}(\theta)$, which has a unique minima at θ_0. In the case of the WFD-R algorithm, it was found that the sequence of estimates, $\{\tilde{\theta}(n)\}_{n=1}^{\infty}$, oscillated wildly around θ_0 and the oscillations tended to get less frequent with increasing L. This could be explained form the observations we have made in this section on the convergence of WFD-R algorithms. As the inputs are ARMA processes, the random variations in the inputs influence $V_L^n(\theta)$, for all n. Hence, for small values of L, the cost functions $V_L^n(\theta)$, may not have a minima close to θ_0 for most iteration instants, *i.e.*, for most values of n. Increasing L tends to suppress the effect of variations in the inputs, thereby leading to $V_L^n(\theta)$'s having a minima close to θ_0 more frequently.

7 Conclusions

In this paper, we analyzed in detail the convergence of the FD-R algorithm and the WFD-R algorithm, which were originally proposed in [5]. Initially, the conditions on the inputs, under which the convergence of the algorithms of were analyzed, included all MA processes. Later they were relaxed to include ARMA processes as well. The convergence analysis presented in this paper also gives a good insight into the working of the algorithm. This is particularly evident form the explanation we have provided for the numerical results obtained in [5]. From a more general perspective, this paper lays a general framework for analyzing the convergence of the recursive algorithms defined in the frequency domain.

8 Appendix

8.1 Uniform convergence of (80)

In this subsection, we will show that the convergence (80) is uniform in θ for all $\theta \in \mathcal{D}$.

Lemma 1. *The convergence*

$$\begin{aligned}
&\lim_{N\to\infty} \frac{\tilde{\boldsymbol{g}}(\theta)^\top}{N-L+1} \sum_{n=L}^{N} \begin{bmatrix} \boldsymbol{u}_{n,L}^{(m)} \boldsymbol{u}_{n,L}^{(m)\top} & \boldsymbol{O}_{(m+1)\times(L-(m+1))} \\ \boldsymbol{O}_{(L-(m+1))\times(m+1)} & \boldsymbol{O}_{(L-(m+1))\times(L-(m+1))} \end{bmatrix} \tilde{\boldsymbol{g}}(\theta) \\
= \;& \tilde{\boldsymbol{g}}(\theta)^\top \begin{bmatrix} \boldsymbol{R}_{uu}(m) & \boldsymbol{O}_{(m+1)\times(L-(m+1))} \\ \boldsymbol{O}_{(L-(m+1))\times(m+1)} & \boldsymbol{O}_{(m+1)\times(m+1)} \end{bmatrix} \tilde{\boldsymbol{g}}(\theta)^\top, \qquad (101)
\end{aligned}$$

see also (80), is uniform in θ for all $\theta \in \mathcal{D}$.

Proof. From Assumption (A2), we know that

$$\begin{aligned}
&\lim_{N\to\infty} \frac{1}{N-L+1} \sum_{n=L}^{N} \begin{bmatrix} \boldsymbol{u}_{n,L}^{(m)} \boldsymbol{u}_{n,L}^{(m)\top} & \boldsymbol{O}_{(m+1)\times(L-(m+1))} \\ \boldsymbol{O}_{(L-(m+1))\times(m+1)} & \boldsymbol{O}_{(L-(m+1))\times(L-(m+1))} \end{bmatrix} \\
= \;& \begin{bmatrix} \boldsymbol{R}_{uu}(m) & \boldsymbol{O}_{(m+1)\times(L-(m+1))} \\ \boldsymbol{O}_{(L-(m+1))\times(m+1)} & \boldsymbol{O}_{((m+1))\times(m+1)} \end{bmatrix}. \qquad (102)
\end{aligned}$$

To show that the convergence (102) is not only point-wise but uniform in θ for all $\theta \in \mathcal{D}$, we use the following matrix inequality involving the 1−norm, see [3]. Let x denote an arbitrary $p \times 1$ vector with real entries and A denote an arbitrary $p \times p$ matrix with real entries, and let $\| \bullet \|_1$ denote the 1−norm, *i.e.*,

$$\| A \|_1 \triangleq \max_{1\le j\le p} \sum_{i=1}^{p} | a_{ij} | \quad \text{(column sum)} \qquad (103)$$

and

$$\| x \|_1 \triangleq \sum_{i=1}^{p} | x_i | \,. \qquad (104)$$

It holds that

$$\begin{aligned}
\| x^\top A x \|_1 &\le \| x^\top \|_1 \| Ax \|_1 \\
&\le \| x \|_1 \| A \|_1 \| x \|_1 \\
&= \| x \|_1^2 \| A \|_1, \qquad (105)
\end{aligned}$$

see pages 29 – 30 of [3] for more details. Further, since $x^\top Ax$ is a scalar, we have

$$| \, x^\top Ax \, | \;\; \leq \;\; \| \, x \, \|_1^2 \| \, A \, \|_1 \, . \tag{106}$$

Setting

$$x \;\; \triangleq \;\; \tilde{\boldsymbol{g}}(\theta) \tag{107}$$

and

$$A \;\; \triangleq \;\; R_N - R, \tag{108}$$

where

$$R_N \;\; \triangleq \;\; \frac{1}{N-L+1} \sum_{n=L}^{N} \begin{bmatrix} \boldsymbol{u}_{n,L}^{(m)} \boldsymbol{u}_{n,L}^{(m)\top} & \boldsymbol{O}_{(m+1)\times(L-(m+1))} \\ \boldsymbol{O}_{(L-(m+1))\times(m+1)} & \boldsymbol{O}_{(L-(m+1))\times(L-(m+1))} \end{bmatrix} \tag{109}$$

and

$$R \;\; \triangleq \;\; \begin{bmatrix} \boldsymbol{R}_{uu}(m) & \boldsymbol{O}_{(m+1)\times(L-(m+1))} \\ \boldsymbol{O}_{(L-(m+1))\times(m+1)} & \boldsymbol{O}_{((m+1))\times(m+1)} \end{bmatrix}, \tag{110}$$

in the inequality (106), we have

$$| \, \tilde{\boldsymbol{g}}(\theta)^\top (R_N - R) \tilde{\boldsymbol{g}}(\theta) \, | \;\; \leq \;\; \| \, \tilde{\boldsymbol{g}}(\theta) \, \|_1^2 \| \, R_N - R \, \|_1 \, . \tag{111}$$

Note that

$$\| \, \tilde{\boldsymbol{g}}(\theta) \, \|_1^2 = \left[\sum_{k=0}^{L-1} | \, \tilde{g}(k,\theta) \, | \right]^2 . \tag{112}$$

Further, as $\mathcal{D}$ is a compact set, see (A1), there exists an $M > 0$, such that

$$\| \, \tilde{\boldsymbol{g}}(\theta) \, \|_1 \;\; \leq \;\; \sqrt{M}, \;\; \forall \;\; \theta \in \mathcal{D} \tag{113}$$

see page 89 of [12]. Since $R_N \to R$ point-wise as $N \to \infty$, for any given $\epsilon > 0$ there exits an integer $K > 0$, such that

$$\| \, R_N - R \, \|_1 \;\; < \;\; \frac{\epsilon}{M}, \;\; N \;\geq\; K. \tag{114}$$

Hence, using (113) and (114) in (111), we have

$$| \, \tilde{\boldsymbol{g}}(\theta)^\top (R_N - R) \tilde{\boldsymbol{g}}(\theta) \, | \;\; < \;\; \epsilon, \;\; N \;\geq\; K, \;\; \forall \, \theta \in \mathcal{D}, \tag{115}$$

which fits the definition of uniform convergence.

This observation completes the proof.

8.2 Convergence of (91)

In this subsection, we will show that

$$\begin{aligned} W(\theta) &= \lim_{L\to\infty} W_L(\theta) \\ &\approx \lim_{L\to\infty} \bar{W}_L^{(2,2)}(\theta), \end{aligned} \tag{116}$$

where

$$\begin{aligned} W_L(\theta) &\approx \bar{W}_L^{(1,1)}(\theta_0) + \bar{W}_L^{(2,2)}(\theta) + \bar{W}_L^{(3,3)}(\theta) \\ &+ 2\bar{W}_L^{(1,2)}(\theta) - 2\bar{W}_L^{(2,3)}(\theta) - 2\bar{W}_L^{(1,3)}(\theta), \end{aligned} \tag{117}$$

with the individual elements $\bar{W}_L^{(1,1)}(\theta_0)$, $\bar{W}_L^{(2,2)}(\theta)$, $\bar{W}_L^{(3,3)}(\theta)$, $\bar{W}_L^{(1,2)}(\theta)$, $\bar{W}_L^{(2,3)}(\theta)$ and $\bar{W}_L^{(1,3)}(\theta)$, as defined in (90). In other words, here, we will show that the terms $\bar{W}_L^{(1,1)}(\theta_0)$, $\bar{W}_L^{(3,3)}(\theta)$, $\bar{W}_L^{(1,2)}(\theta)$, $\bar{W}_L^{(2,3)}(\theta)$ and $\bar{W}_L^{(1,3)}(\theta)$ converge to zero as $L \to \infty$, for all $\theta \in \mathcal{D}$. To avoid repetition, we will only show that $\bar{W}_L^{(1,1)}(\theta)$ converges to zero, as $L \to \infty$, for all θ in $\mathcal{D}$. Convergence proofs for the other terms, $\bar{W}_L^{(3,3)}(\theta)$, $\bar{W}_L^{(1,2)}(\theta)$, $\bar{W}_L^{(2,3)}(\theta)$ and $\bar{W}_L^{(1,3)}(\theta)$, run in similar lines to the convergence proof provided for the term $\bar{W}_L^{(1,1)}(\theta)$.

We prove the convergence of $\bar{W}_L^{(1,1)}(\theta_0)$ to zero, in a sequence of lemmas.

Lemma 2. *If $\{a_m\}_{m=0}^{\infty}$ is a sequence of real numbers such that*

$$\lim_{m\to\infty} a_m = a^* \tag{118}$$

then the sequence

$$U_L \triangleq \frac{1}{L}\sum_{m=0}^{L-1} a_m, \quad L = 0, 1, 2, \ldots, \tag{119}$$

also converges to a^*, as $L \to \infty$.

Proof. Choose an arbitrary $\epsilon > 0$. Since

$$\lim_{m\to\infty} a_m = a^*, \tag{120}$$

there exists an L^* such that

$$| \, a_m - a^* \, | < \frac{\epsilon}{2} \ \forall \ m \geq L^*. \tag{121}$$

Consider $\mid U_L - a^* \mid$. Note that

$$\begin{aligned} \mid U_L - a^* \mid &= \mid \frac{1}{L}\sum_{m=0}^{L-1} a_m - a^* \mid = \mid \frac{1}{L}\sum_{m=0}^{L-1}(a_m - a^*) \mid \\ &\leq \frac{1}{L}\sum_{m=0}^{L-1} \mid a_m - a^* \mid . \end{aligned} \tag{122}$$

Let $L > L^*$, where L^* is as in (121). Splitting the sum in the RHS of (122), and using (121), we get

$$\begin{aligned} \mid U_L - a^* \mid &\leq \frac{1}{L}\sum_{m=0}^{L^*-1} \mid a_m - a^* \mid + \frac{1}{L}\sum_{m=L^*}^{L-1} \mid a_m - a^* \mid \\ &\leq \frac{1}{L}\sum_{m=0}^{L^*-1} \mid a_m - a^* \mid + \frac{\epsilon}{2} \\ &\leq \epsilon, \end{aligned} \tag{123}$$

if L is chosen large enough. More specifically, if

$$L \geq \max\left(L^*, \frac{2}{\epsilon}\sum_{m=0}^{L^*-1} \mid a_m - a^* \mid\right).$$

This completes our proof.

Lemma 3. *The sum*

$$\begin{aligned} & W_L^{(1,1)}(\theta) \\ = & \frac{1}{L}\sum_{m=0}^{L-1} \boldsymbol{g}^\top(\theta) \begin{bmatrix} \boldsymbol{O}_{(m+1)\times(m+1)} & \boldsymbol{O}_{(m+1)\times(L-(m+1))} \\ \boldsymbol{O}_{(m+1)\times(L-(m+1))} & \boldsymbol{R}_{\psi\psi}(m) \end{bmatrix} \boldsymbol{g}(\theta), \end{aligned} \tag{124}$$

$\forall\ \theta \in \mathcal{D}$, see (90), converges to zero as $L \to \infty$.

Proof. Consider the general term

$$S_m \triangleq \boldsymbol{g}^\top(\theta) \begin{bmatrix} \boldsymbol{O}_{(m+1)\times(m+1)} & \boldsymbol{O}_{(m+1)\times(L-(m+1))} \\ \boldsymbol{O}_{(m+1)\times(L-(m+1))} & \boldsymbol{R}_{\psi\psi}(m) \end{bmatrix} \boldsymbol{g}(\theta), \tag{125}$$

in the finite sum $W_L^{(1,1)}(\theta)$, (124). Since

$$\boldsymbol{g}(\theta) = \begin{bmatrix} g_{H_d}(0,\theta) & g_{H_d}(1,\theta) & \ldots & g_{H_d}(L-1,\theta) \end{bmatrix}^\top, \tag{126}$$

see (61), (125) simplifies to

$$S_m = \boldsymbol{g}_{T,m}^{\top}(\theta)\boldsymbol{R}_{\psi\psi}(m)\boldsymbol{g}_{T,m}(\theta), \tag{127}$$

where

$$\boldsymbol{g}_{T,m}(\theta) \triangleq \begin{bmatrix} g_{H_d}(m+1,\theta) & g_{H_d}(m+2,\theta) & \dots & g_{H_d}(L-1,\theta) \end{bmatrix}^{\top}. \tag{128}$$

As a consequence of Lemma 2, to prove

$$\lim_{L\to\infty} W_L^{(1,1)}(\theta) = 0, \tag{129}$$

it is enough to show that

$$\lim_{m\to\infty} S_m = 0. \tag{130}$$

In the rest of the proof, we will show that (130) holds.

Since S_m, (127), is a scalar, we have as in (106)

$$\begin{aligned} \mid S_m \mid &= \parallel \boldsymbol{g}_{T,m}^{\top}(\theta)\boldsymbol{R}_{\psi\psi}(m)\boldsymbol{g}_{T,m}(\theta) \parallel_1 \\ &\leq \parallel \boldsymbol{g}_{T,m}(\theta) \parallel_1^2 \ \parallel \boldsymbol{R}_{\psi\psi}(m) \parallel_1 . \end{aligned} \tag{131}$$

Using the definition of 1$-$norm for a vector, see (104), it holds that

$$\parallel \boldsymbol{g}_{T,m}(\theta) \parallel_1 = \sum_{k=m+1}^{L-1} \mid g_{H_d}(k,\theta) \mid . \tag{132}$$

In the case of $\parallel \boldsymbol{R}_{\psi\psi}(m) \parallel_1$, we know from (78) that

$$\boldsymbol{R}_{\psi\psi}(m) = \begin{bmatrix} r(0) & r(1) & \dots & r(L-(m+2)) \\ r(1) & r(0) & \dots & r(L-(m+3)) \\ \vdots & \vdots & \ddots & \vdots \\ r(L-(m+2)) & r(L-(m+3)) & \dots & r(0) \end{bmatrix}. \tag{133}$$

Using the definition of a 1$-$norm for a matrix, see (103), and Assumption (A3), $\boldsymbol{R}_{\psi\psi}(m)$ can easily be bounded. More specifically as

$$[\boldsymbol{R}_{\psi\psi}(m)]_{ij} = r(\mid i-j \mid), \tag{134}$$

it holds that

$$\begin{aligned}
\| \boldsymbol{R}_{\psi\psi}(m) \|_1 &= \max_j \sum_i \mid [\boldsymbol{R}_{\psi\psi}(m)]_{ij} \mid \\
&= \max_j \left[\sum_{i=0}^{L-(m+1)} \mid r(i-j) \mid \right] \\
&\leq \max_{1 \leq j \leq L-(m+1)} \left[\sum_{k=-N_1}^{N_1} \mid r(k) \mid \right] \\
&\leq 2 \sum_{k=0}^{N_1} \mid r(k) \mid \\
&\triangleq r_{\max} \qquad (135)
\end{aligned}$$

which is finite. Since

$$\sum_{k=0}^{\infty} \mid g_{H_d}(k, \theta) \mid \; < \; \infty, \;\; \forall\, \theta \; \in \; \mathcal{D} \qquad (136)$$

invoking the Cauchy criterion for a convergent series, see page 59 of [12], given an $\epsilon \; > \; 0$ there exists an L^* such that

$$\sum_{k=m}^{L-1} \mid g_{H_d}(k, \theta) \mid \; < \; \sqrt{\frac{\epsilon}{r_{\max}}} \;\; \forall \;\; L \geq m > L^*, \;\; \theta \; \in \; \mathcal{D}. \qquad (137)$$

Using (135) and (137) in (131), we get

$$\mid S_m \mid \; < \; \epsilon \;\; \forall \;\; L \geq m > L^*. \qquad (138)$$

This proves (130), and hence the claim of the lemma.

8.3 Proof of (93)

In this subsection, we will show that the limit

$$\bar{W}^{(2,2)}(\theta) = \lim_{L \to \infty} \bar{W}_L^{(2,2)}(\theta) \qquad (139)$$

see (93), is strictly positive for all $\theta \in \mathcal{D}$ and $\theta \neq \theta_0$.

Lemma 4. *The limit*

$$\bar{W}^{(2,2)}(\theta) = \lim_{L \to \infty} \bar{W}_L^{(2,2)}(\theta), \qquad (140)$$

where

$$\begin{aligned} &\bar{W}_L^{(2,2)}(\theta) \\ = \;& \frac{1}{L}\sum_{m=0}^{L-1} \tilde{\boldsymbol{g}}(\theta)^\top \begin{bmatrix} \boldsymbol{R}_{uu}(m) & \boldsymbol{O}_{m+1\times(L-(m+1))} \\ \boldsymbol{O}_{(L-(m+1))\times(m+1)} & \boldsymbol{O}_{(L-(m+1))\times(L-(m+1))} \end{bmatrix} \tilde{\boldsymbol{g}}(\theta), \end{aligned} \tag{141}$$

is strictly positive for all $\theta \in \mathcal{D}$ and $\theta \neq \theta_0$.

Proof. Consider the general term

$$T_m \triangleq \tilde{\boldsymbol{g}}(\theta)^\top \begin{bmatrix} \boldsymbol{R}_{uu}(m) & \boldsymbol{O}_{m+1\times(L-(m+1))} \\ \boldsymbol{O}_{(L-(m+1))\times(m+1)} & \boldsymbol{O}_{(L-(m+1))\times(L-(m+1))} \end{bmatrix} \tilde{\boldsymbol{g}}(\theta), \tag{142}$$

in the finite sum (141). From (61) and (72) we know that

$$\tilde{\boldsymbol{g}}(\theta)^\top = \begin{bmatrix} \tilde{g}_{H_d}(0,\theta) & \tilde{g}_{H_d}(1,\theta) & \dots & \tilde{g}_{H_d}(L-1,\theta) \end{bmatrix}^\top, \tag{143}$$

where

$$\tilde{g}_{H_d}(k,\theta) = g_{H_d}(k,\theta_0) - g_{H_d}(k,\theta), \quad k = 0,1,2,\dots,L-1. \tag{144}$$

Hence T_m, (142), simplifies to

$$T_m = \tilde{\boldsymbol{g}}_{U,m}(\theta)^\top \boldsymbol{R}_{uu}(m) \tilde{\boldsymbol{g}}_{U,m}(\theta), \tag{145}$$

where

$$\tilde{\boldsymbol{g}}_{U,m}(\theta) = \begin{bmatrix} \tilde{g}_{H_d}(0,\theta) & \tilde{g}_{H_d}(1,\theta) & \dots & \tilde{g}_{H_d}(m,\theta) \end{bmatrix}^\top. \tag{146}$$

From Lemma 2 we know that, to show $\bar{W}^{(2,2)}(\theta) > 0$, for all $\theta \neq \theta_0$, it is enough to show that

$$T \triangleq \lim_{m\to\infty} T_m > 0 \;\forall\; \theta \neq \theta_0 \tag{147}$$

Since $\boldsymbol{R}_{uu}(m)$ is a symmetric matrix, which is strictly positive definite due to assumption (A3), we have

$$0 < \lambda_{min}(\boldsymbol{R}_{uu}(m)) M_m \leq T_m \leq \lambda_{max}(\boldsymbol{R}_{uu}(m)) M_m \tag{148}$$

where $\lambda_{min}(\boldsymbol{R}_{uu}(m))$ and $\lambda_{max}(\boldsymbol{R}_{uu}(m))$ denote the maximum and minimum eigenvalues, respectively, of $\boldsymbol{R}_{uu}(m)$ and

$$M_m = \sum_{k=0}^{m} \left[\tilde{g}_{H_d}(k,\theta)\right]^2. \tag{149}$$

Note that

$$\lim_{m\to\infty} M_m = \sum_{k=0}^{\infty} [\tilde{g}_{H_d}(k,\theta)]^2$$
$$\triangleq M, \tag{150}$$

exists and is strictly positive for $\theta \neq \theta_0$. Hence,

$$T \geq M \lim_{m\to\infty} \lambda_{min}(\boldsymbol{R}_{uu}(m)). \tag{151}$$

If

$$\lim_{m\to\infty} \lambda_{min}(\boldsymbol{R}_{uu}(m)) > 0, \tag{152}$$

then it is evident that

$$T > 0. \tag{153}$$

However, inspite of the fact that $\boldsymbol{R}_{uu}(m))$ is positive definite for all $m = 0, 1, 2, \ldots$, in certain rare cases it is possible that

$$\lim_{m\to\infty} \lambda_{min}(\boldsymbol{R}_{uu}(m)) = 0. \tag{154}$$

Implying

$$T \geq 0, \tag{155}$$

and thereby leaving the option of $T = 0$ open. To show that (153) holds even if (154) were to happen, we use the following remarkable and well known result presented in [10]. Let

$$\mathbf{v}_N(\omega) \triangleq \begin{bmatrix} 1 & e^{\mathrm{i}\omega} & e^{2\mathrm{i}\omega} & \ldots & e^{(N-1)\mathrm{i}\omega} \end{bmatrix}^\top \tag{156}$$

Under the assumption (A3), it shown that for a large N, see [10],

$$\mathbf{R}_{uu}(N)\mathbf{v}_N(\omega) \approx \phi_u(\omega)\mathbf{v}_N(\omega), \tag{157}$$

where $\phi_u(\omega)$ is the spectral density of the input $u(t)$ at ω, with the approximation involved tending to an equality as $N \to \infty$. It is worth mentioning that, (157) is due the fact that $\mathbf{R}_{uu}(N)$ is close to a circulant matrix for a large N.

For simplicity, assume that only one of the eigenvalues of $\mathbf{R}_{uu}(m)$ converges to zero as $m \to \infty$, in which case there exists exactly one frequency point ω_1, such that $\phi_u(\omega_1) = 0$, with $\lim_{m\to\infty} \mathbf{v}_m(\omega_1)$ denoting the eigenvector corresponding to the limiting zero eigenvalue. Alternatively, in terms of approximations, for a large N

$$\lambda_{\min}(\mathbf{R}_{uu}(N)) \;\approx\; \phi_u(\omega_1) \;=\; 0 \tag{158}$$

and

$$\mathbf{R}_{uu}(N)\mathbf{v}_N(\omega_1) \;\approx\; 0. \tag{159}$$

If

$$T \;=\; \lim_{m\to\infty} T_m \;=\; 0, \tag{160}$$

then (145) implies that

$$\mathbf{R}_{uu}(N)\tilde{\boldsymbol{g}}_{U,N}(\theta) \;\approx\; 0, \tag{161}$$

which inturn implies

$$\tilde{\boldsymbol{g}}_{U,N}(\theta) \;\approx\; \alpha\mathbf{v}_N(\omega_1), \tag{162}$$

for some constant α. In words, $\tilde{\boldsymbol{g}}_{U,N}(\theta)$ approximately lies in the in eigenspace corresponding to the smallest eigenvalue, (158). Note that (162) is a contradiction, as we know that the elements $\tilde{g}_{H_d}(k,\theta)$, (144), of vector $\tilde{\boldsymbol{g}}_{U,N}(\theta)$, converge to zero as the index k increases, but the elements of $\mathbf{v}_N(\omega_1)$ are all of constant magnitude equal to one. Hence $\tilde{\boldsymbol{g}}_{U,N}(\theta)$ in the limiting case cannot lie in the eigenspace corresponding to the limiting zero eigenvalue, which rules out the possibility of (160). The above arguments can be extended to the case where $\mathbf{R}_{uu}(m)$ has a finite number of eigenvalues converging to zero.

This completes the proof.

References

[1] H. Kwakernaak and R. Sivan. *Modern Signals and Systems.* Prentice Hall, New Jersy, 1991.

[2] J. Schoukens, R. Pintelon and H. Van Hamme. Identification of linear dynamic systems using piecewise constant excitations: use, misuse and alternatives. *Automatica*, 1994. Vol. 30, No. 7, pp 1153-1169.

[3] K. Zhou with J. C. Doyle and K. Glover. *Robust and Optimal Control.* Prentice Hall, New Jersy, 1995.

[4] R. Pintelon and J. Schoukans. *System Identification: A Frequency Domain Approach.* IEEE Press, Piscataway, NJ, 2001.

[5] B. Bhikkaji, T. Söderström and K. Mahata. Recursive algorithms for estimating the parameters in a one dimensional heat diffusion system: derivation and implementation. *Submitted for publication.*

[6] B. Bhikkaji. Reduced Order Models for Diffusion Systems. *Licentiate thesis, Department of Information Technology, Uppsala University, Uppsala*, 2000.

[7] B. Bhikkaji and T. Söderström. Bias and Variance of The Parameter Estimates for A One Dimensional Heat Diffusion System. *Accepted for Publication in the Proc of 15th IFAC Congress*, 2002. Barcelona, Spain, June.

[8] B. Bhikkaji and T. Söderström. Recursive algorithm for estimating the parameters in one dimensional heat diffusion system. *Reglermöte*, 2002. Linköping, Sweden, 20-30 May.

[9] A.V. Oppenheim and R.W. Schafer. *Discrete-Time Signal Processing.* Printice Hall-Inc, New Jersey, 1975.

[10] R. M. Gray. On the asymptotic eigenvalue distribution of Toeplitz matrices. *IEEEE Transactions on Information Theory*, 1972. Vol. 18:6, pp. 725-730.

[11] S. Remle. Modeling and Parameter Estimation of the Diffusion Equation. *Licentiate thesis, Department of Information Technology, Uppsala University, Uppsala*, 2000.

[12] W. Rudin. *Principles of Mathematical Analysis.* McGraw-Hill International, Singapore, 1976.

[13] S. K. Mitra and J. F. Kaiser. *Handbook for Digital Signal Processing.* John Wiley and Sons, New York, 1993.

[14] T. Söderström and B. Bhikkaji. Reduced Order Models for Diffusion Systems via Collocation Methods. *Proc of 12th IFAC Symposium on System Identification*, 2000. Santa Barbara, CA, 21-23 June.

[15] T. Söderström and S. Remle. Parameter Estimation for Diffusion Models. *Proc of 12th IFAC Symposium on System Identification*, 2000. Santa Barbara, CA, 21-23 June.

[16] T. Söderström and P. Stoica. *System Identification.* Prentice Hall International, Hemel Hempstead, UK, 1989.